Natural Resources Canada
Ressources naturelles Canada

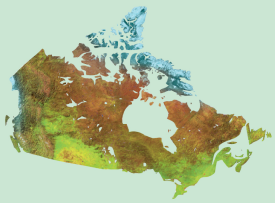

Geological Survey of Canada
Bulletin 615

Targeted Geoscience Initiative 5: Integrated multidisciplinary studies of unconformity-related uranium deposits from the Patterson Lake corridor, northern Saskatchewan

E.G. Potter, V. Tschirhart, J.W. Powell, C.J. Kelly, M. Rabiei, D. Johnstone, J.A. Craven, W.J. Davis, S. Pehrsson, S.M. Mount, G. Chi, and K.M. Bethune

2020

Canada

Geological Survey of Canada
Bulletin 615

Targeted Geoscience Initiative 5: Integrated multidisciplinary studies of unconformity-related uranium deposits from the Patterson Lake corridor, northern Saskatchewan

E.G. Potter, V. Tschirhart, J.W. Powell, C.J. Kelly,
M. Rabiei, D. Johnstone, J.A. Craven, W.J. Davis,
S. Pehrsson, S.M. Mount, G. Chi, and K.M. Bethune

2020

ISSN 2560-7219
ISBN 978-0-660-34891-9
Catalogue No. M42-615E-PDF
https://doi.org/10.4095/326040

A copy of this publication is also available for reference in depository libraries across Canada through access to the Depository Services Program's Web site at http://dsp-psd.pwgsc.gc.ca.

This publication is available for free download through GEOSCAN (https://geoscan.nrcan.gc.ca).

Recommended citation

Potter, E.G., Tschirhart, V., Powell, J.W., Kelly, C.J., Rabiei, M., Johnstone, D., Craven, J.A., Davis, W.J., Pehrsson, S., Mount, S.M., Chi, G., and Bethune, K.M., 2020. Targeted Geoscience Initiative 5: Integrated multidisciplinary studies of unconformity-related uranium deposits from the Patterson Lake corridor, northern Saskatchewan; Geological Survey of Canada, Bulletin 615, 37 p. https://doi.org/10.4095/326040

Cover illustration
Fine-grained uraninite precipitated along a chemical front between hematite-rich and clay- plus tourmaline-rich zones. Drillhole AR-16-78c1, at 467.5 m depth. NRCan Photo 2019-788, Photograph by E.G. Potter. NRCan photo 2019-788 (detail)

Critical review
G. Zaluski
T. Peterson

Authors

E.G Potter (eric.potter@canada.ca)
V. Tschirhart
(victoria.tschirhart@ canada.ca)
J.W. Powell (jeremy.powell@canada.ca)
C.J. Kelly (colter.kelly@canada.ca)
J.A. Craven (jim.craven@canada.ca)
W.J. Davis (bill.davis@canada.ca)
S. Pehrsson (sally.pehrsson@canada.ca)
Geological Survey of Canada
601 Booth Street
Ottawa, Ontario
K1A 0E8

M. Rabiei (rabeiemorteza@gmail.com)
D. Johnstone
(dillon.johnstone@gov.sk.ca)
G. Chi (Guoxiang.Chi@uregina.ca)
K.M. Bethune
(kathryn.bethune@uregina.ca)
University of Regina
Department of Geology
3737 Wascana Parkway
Regina, Saskatchewan
S4S 0A2

D. Johnstone
(dillon.johnstone@gov.sk.ca)
Also at:
Saskatchewan Geological Survey
1000, 2103 - 11th Avenue
Regina, Saskatchewan
S4P 3Z8

S.M. Mount
(SarahMount@cmail.carleton.ca)
Carleton University
Department of Earth Sciences
1125 Colonel By Drive
Ottawa, Ontario
K1S 5B6

CONTENTS

Figures

Targeted Geoscience Initiative 5: Integrated multidisciplinary studies of unconformity-related uranium deposits from the Patterson Lake corridor, northern Saskatchewan

Abstract: Basement-hosted uranium deposits of the Patterson Lake corridor are located on the southwestern margin of the Athabasca Basin in atypical hosts: altered and metamorphosed granite, granodiorite, and ultramafic to mafic rocks. Fluid inclusions record incursion of two fluids, NaCl- and $CaCl_2$-dominant, at temperatures up to 250°C and approximately 1 km into the basement during episodic brittle reactivation of high-strain–ductile to brittle-ductile structures, in particular late west- and north-northwest–striking brittle conjugate faults that crosscut the Athabasca sandstone. Isotopic data from pyrite and tourmaline record basinal fluid-rock interactions under fluctuating pressure and oxidizing to reducing conditions. New 3-D geophysical modelling illustrates linkages between the surface architecture and lower crust to mantle and influence of the Clearwater Domain granitic intrusions on the ore systems. High radiogenic heat production from these intrusions and other ca. 1.8 Ga felsic intrusions contributed to a prolonged, elevated geothermal gradient under the Proterozoic basins that permitted shallow (less than 3 km) depths of mineralization.

Résumé : Les gisements d'uranium encaissés dans le socle du corridor du lac Patterson sont situés à la bordure sud-ouest du bassin d'Athabasca dans des roches hôtes atypiques : granite, granodiorite et roches ultramafiques à mafiques altérés et métamorphisés. Les inclusions fluides rendent compte de l'infiltration de deux fluides, à prédominance de NaCl pour l'un et de $CaCl_2$ pour l'autre, à des températures aussi élevées que 250 °C et à une profondeur d'environ 1 km dans le socle, pendant des épisodes de réactivation en mode fragile de structures ductiles de forte déformation en structures fragiles-ductiles, plus particulièrement les failles fragiles conjuguées de directions ouest et nord–nord-ouest de formation tardive qui recoupent les grès d'Athabasca. Les données isotopiques de la pyrite et de la tourmaline font état d'interactions entre les fluides de bassin et les roches dans des conditions fluctuantes de pression ainsi que d'oxydation et de réduction. Une nouvelle modélisation géophysique 3D révèle des liens entre l'architecture de surface et l'interface croûte inférieure/manteau, ainsi que l'incidence des intrusions granitiques du domaine de Clearwater sur les systèmes minéralisateurs. La forte chaleur radiogénique produite par ces intrusions et d'autres intrusions felsiques datant d'environ 1,8 Ga a contribué à l'existence d'un gradient géothermique élevé de longue durée dans les bassins du Protérozoïque, ce qui a permis la mise en place de minéralisations à faible profondeur (à moins de 3 km).

SUMMARY

The Athabasca Basin contains the highest-grade uranium deposits in the world. Discovered in the late 1960s, exploration has mainly focused on the eastern margin of the basin where the deposits are associated with the basin-basement unconformity and graphite-rich basement faults rooted in metapelitic gneisses. In contrast, newly discovered deposits of the Patterson Lake corridor located on the southwestern margin of the basin are hosted within altered, metamorphosed granite, granodiorite, and ultramafic to mafic basement rocks. Similar to deposits in the eastern portion of the basin, primary, pseudosecondary, and secondary fluid inclusions in quartz veins from Patterson Lake corridor deposits record two fluid compositions, NaCl- and $CaCl_2$-rich, with total homogenization temperatures ranging from 80 to 250°C and no significant temporal or spatial variations. The coexistence of liquid-dominated, vapour-dominated, and vapour-only fluid inclusions in fluid inclusion assemblages from barren and mineralized zones suggests fluid boiling occurred during mineralization; however, under normal geothermal gradients, fluids of these compositions cannot boil at the temperatures indicated by the fluid inclusion data. The only mechanism to explain boiling under these conditions is by faulting which causes rapid changes in pressure. Fluid inclusion analyses and boron isotopic composition of hydrothermal tourmaline support incursion of uranium-bearing basin brines up to 1 km into the basement during episodic brittle reactivation of high-strain ductile to brittle-ductile structures, in particular late west- and north-northwest–striking brittle conjugate faults that crosscut the Athabasca sandstone. Isotopic data from pyrite record significant fluid-rock interactions and element recycling during fluctuating oxidized and reduced conditions along the reactivated fault zones. Although the geological settings and extension of mineralization up to 1 km below the unconformity differ from the classical models, these results support classification of the Patterson Lake corridor deposits as 'unconformity related'.

New 3-D geophysical modelling of the buried basement rocks illustrates linkages between the surface architecture and lower crust/mantle and in particular, highlight the influence of the Clearwater Domain granitic intrusions on the ore systems. Preliminary geochemistry and geochronology

SOMMAIRE

Le bassin d'Athabasca renferme les gisements d'uranium les plus riches au monde, dont la découverte remonte à la fin des années 1960. L'exploration a été concentrée surtout à la bordure orientale du bassin, où les gisements sont associés à la discordance séparant la succession de bassin du socle et à des failles riches en graphite qui s'enfoncent dans des gneiss métapélitiques du socle. En revanche, les gisements récemment découverts dans le corridor du lac Patterson, situé à la bordure sud-ouest du bassin, sont encaissés dans des roches altérées et métamorphisées du socle composées de granite, de granodiorite et de roches ultramafiques à mafiques. Comme dans les gisements de la partie orientale du bassin, les inclusions fluides primaires, pseudo-secondaires et secondaires dans les filons de quartz des gisements du corridor du lac Patterson renferment des fluides de deux compositions, l'une riche en NaCl et l'autre en $CaCl_2$, et affichent des températures d'homogénéisation totale allant de 80 à 250 °C, sans que l'on observe de variations temporelles ou spatiales d'importance. La coexistence d'inclusions fluides à phase liquide dominante, à phase vapeur dominante et à phase vapeur seule dans des assemblages d'inclusions fluides provenant de zones stériles et de zones minéralisées indique qu'une ébullition des fluides s'est produite au cours de la minéralisation. Cependant, dans des gradients géothermiques normaux, les fluides affichant de telles compositions ne peuvent pas bouillir aux températures indiquées par les données sur les inclusions fluides. Le seul mécanisme permettant d'expliquer une ébullition dans ces conditions est la formation de failles qui provoque des changements rapides de pression. Les analyses des inclusions fluides et la composition isotopique du bore dans les tourmalines hydrothermales étayent l'incursion de saumures de bassin uranifères jusqu'à 1 km dans le socle pendant des épisodes de réactivation en mode fragile de structures ductiles de forte déformation en structures fragiles-ductiles, plus particulièrement les failles fragiles conjuguées de directions ouest et nord-nord-ouest de formation tardive, qui recoupent les grès d'Athabasca. Les données isotopiques de la pyrite font état d'importantes interactions fluide-roche et d'un recyclage des éléments dans des conditions fluctuantes d'oxydation et de réduction le long des zones de failles réactivées. Bien que le cadre géologique et le prolongement de la minéralisation jusqu'à 1 km sous la discordance diffèrent des modèles classiques, ces résultats viennent étayer la classification des gisements du corridor du lac Patterson comme étant des « gîtes associés à une discordance ».

Une nouvelle modélisation géophysique 3D des roches du socle enfouies montre des liens entre l'architecture de surface et l'interface croûte inférieure/manteau et met notamment en évidence l'influence des intrusions granitiques du domaine de Clearwater sur les systèmes minéralisateurs. Les données géochimiques et géochronologiques préliminaires indiquent

indicate the high-heat–producing Clearwater intrusions were emplaced ca. 1840 Ma. High radiogenic heat production from these intrusions and other ca. 1.8 Ga felsic intrusions beneath the basin (e.g. the Hudson suite, Trans-Hudson Orogen pegmatites and plutons) developed a prolonged, elevated geothermal gradient in the Proterozoic basins, as indicated in thermochronological modelling. These results support a revised genetic model in which hydrothermal mineralization occurred at shallower depths than originally proposed for unconformity-related deposits as a result of the fractured, high-heat–producing intrusions. Brittle-fault reactivations focused oxidized basin brines into the basement rocks, where pressure-induced fluid boiling coupled with fluid-rock interactions caused precipitation of the metals.

que les intrusions de Clearwater, qui ont produit une chaleur élevée, ont été mises en place vers 1840 Ma. La forte chaleur radiogénique produite par ces intrusions et d'autres intrusions felsiques datant d'environ 1,8 Ga sous le bassin (p. ex. la suite d'Hudson, les pegmatites et les plutons de l'orogène trans-hudsonien) a généré un gradient géothermique élevé de longue durée dans les bassins du Protérozoïque, comme l'indique la modélisation thermochronologique. Ces résultats soutiennent un modèle génétique révisé dans lequel la minéralisation hydrothermale des gîtes associés à une discordance se produit à des profondeurs plus faibles que celles proposées à l'origine, en raison de l'existence d'intrusions fracturées produisant une forte chaleur. Les réactivations de failles fragiles ont focalisé les saumures oxydées de bassin dans les roches du socle, où une ébullition des fluides induite par une chute de pression, associée aux interactions entre les fluides et les roches, a provoqué la précipitation des métaux.

INTRODUCTION

The Athabasca Basin remains the primary exploration target for uranium in Canada, hosting the highest-grade deposits in the world. Within the Proterozoic basin and surrounding basement rocks, known uranium deposits are spatially associated with structural trends and/or intersections of crustal-scale faults that are considered the main fluid conduits during formation of the unconformity-related uranium deposits (Jefferson et al., 2007). Many of these structures exhibit multiple generations of deformation (e.g. brittle fabrics overprinting ductile fabrics) and alteration (illite, kaolinite, sudoite, tourmaline, aluminum-phosphate-sulfate minerals, iron oxides, and hydroxides) that generate unique geophysical and geochemical signatures. Under the Targeted Geoscience Initiative (TGI) program, this study examined the role of reactivated, regional-scale faults in the formation of unconformity-related uranium deposits and expressions of fertile alteration along such fluid pathways. The project was focused in the Patterson Lake corridor of northwestern Saskatchewan (Fig. 1), a new exploration district defined by recent high-grade discoveries (e.g. Triple R, Arrow, Harpoon, Cannon, and Spitfire; Ross, 2015; Cox et al., 2017). In the Patterson Lake corridor, known mineralization occurs in reactivated basement structures outside and along the southwestern margin of the Athabasca Basin, with high-grade ore lenses situated well below the basin-basement unconformity in atypical host rocks — indicating the structures were likely significant vertical and horizontal fluid pathways.

REGIONAL AND LOCAL GEOLOGY

The region has a complex geological history, spanning the Mesoarchean (3.0 Ga) to the Mesoproterozoic (1.2 Ga). Located along the southern margin of Athabasca Basin in the Rae Province, Taltson Domain rocks occur to the west and south of the Patterson Lake corridor. Although the northern extent of the Patterson Lake corridor is covered by the basin, exposures of the adjacent Tantato, Beaverlodge, and Zemlak domains occur to the north (Fig. 1). The Tantato Domain is a composite domain divided into three subdomains (Hanmer et al., 1991, 1992, 1994; Snoeyenbos et al., 1997). The Northwestern and Upper Deck subdomains are composed of Neoarchean metagranitoids, psammopelitic gneisses, and mafic granulites (Hanmer, 1997) that experienced high-grade metamorphic conditions at 2.6 to 2.55 Ga and approximately 1.9 Ga (Mahan et al., 2008; Dumond et al., 2010, 2015), whereas the Chipman subdomain consists of ca. 3.41 to 3.14 Ga metatonalite (Hanmer et al., 1994; Hanmer, 1997) and numerous younger metadiabase intrusions deformed and metamorphosed to granulite facies at 1.9 Ga (Flowers et al., 2006a; Mahan et al., 2008; Regan et al., 2014). To the west, the Beaverlodge Domain includes Archean orthogneisses and granitoids and younger Paleoproterozoic dominantly sedimentary rocks such as the ca. 2.3 to 2.1 Ga Murmac Bay Group (Ashton et al., 2013) and the ca. 1.83 to 1.818 Ga Martin Group (Morelli et al., 2009). At least three distinct granitoid suites, dated between 3.0 Ga and 2.29 Ga (Koster and Baadsgaard, 1970; van Schmus et al., 1986; Hartlaub et al., 2004, 2005, 2007), have been recognized in the Beaverlodge Domain and were deformed and metamorphosed along with younger cover during 1940 to 1900 Ma tectonometamorphism (Bethune et al., 2013). West of Beaverlodge, the Zemlak Domain is postulated to be an eastward continuation of the Taltson Domain based on Sm-Nd and U-Pb ages (Ashton et al., 2014). The Zemlak Domain consists of predominantly Archean to Paleoproterozoic orthogneisses deformed together with rare paragneiss (Card et al., 2007a, b), intruded by four suites of granites ranging in age from 2.71 to 2.33 Ga (Ashton et al., 2017) and overlain by metasedimentary rocks of the ca. 1.92 to 1.82 Ga Thluicho Lake Group (Card et al., 2007a, b; Bethune et al., 2010).

The redefined Taltson Domain (Stern et al., 2003; Pană et al., 2007; Card et al., 2014; Powell et al., 2018a), includes the Taltson basement complex and superimposed Taltson magmatic zone. The Taltson basement complex consists predominantly of granulite or retrograded granulite facies and lithologically diverse, 3.2 to 2.1 Ga orthogneisses (McNicoll et al., 2000) with lesser 2.13 to 2.09 Ga Rutledge River paragneiss (Bostock et al., 1991; Bostock and van Breemen, 1994; McNicoll et al., 2000). It extends from the Northwest Territories across the Saskatchewan border and the Snowbird tectonic zone to northeastern Alberta (Card, 2016). The Taltson magmatic zone extends south from the Northwest Territories through northeastern Alberta and continues to the southeast beneath the southwest Athabasca Basin (Pană et al., 2007) to the Snowbird tectonic zone (Fig. 1). The Taltson magmatic zone consists of 1.99 to 1.96 Ga dioritic to granodioritic plutons and 1.95 to 1.92 Ga granites intruded during peak granulite-facies metamorphism (McDonough et al., 2000; McNicoll et al., 2000; Stern et al., 2003; Card et al., 2014; Powell et al., 2018a). To the east of the Patterson Lake corridor, the Virgin River shear zone is the southernmost segment of the Snowbird tectonic zone and is the boundary between the Rae and Hearne provinces (Hanmer et al., 1995; Fig. 1).

The curvilinear Clearwater Domain (Fig. 1, 2a) is a prominent aeromagnetic high and gravity low that divides the Taltson Domain south of the Athabasca Basin

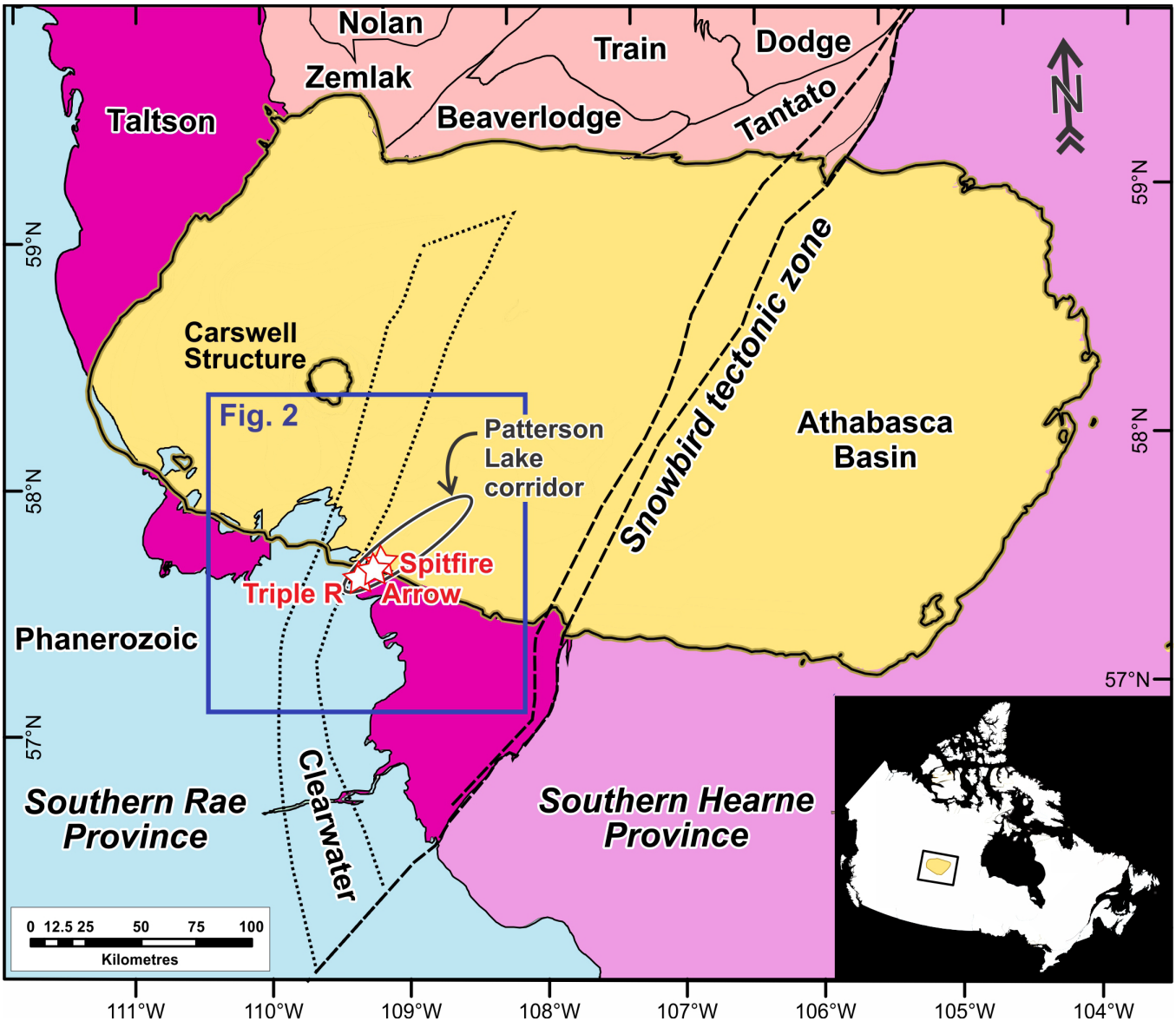

Figure 1. Geological domains underlying the Patterson Lake Corridor hosting the Triple R, Arrow, and Spitfire deposits (stars) and Athabasca Basin in Canada (inset) (*after* Tschirhart et al., 2020).

into eastern and western segments. This poorly exposed terrane consists of a suite of 1843 ± 4 Ma granitoid intrusions (Stern et al., 2003) emplaced during a continental extensional event (Card et al., 2007a), overlapping with emplacement of the Hudson suite granites and formation of early Dubawnt Supergroup basins to the northeast (Peterson et al., 2002; Card, 2018). To the south, across central Alberta, temporally correlative (ca. 1.79–1.85 Ga) Rimbey Arc granitoids lie along the southern margin of the Snowbird tectonic zone (Ross, 2002) and have been interpreted as a magmatic arc related to late accretion of southwestern Hearne to southernmost Rae and Buffalo-Head-Wabamun domains (Ross et al., 2000; Bouzidi et al., 2002; Ross, 2002).

As noted above, the northeastern portion of the Patterson Lake corridor is covered by the Athabasca Basin, which comprises a series of unconformity-bounded clastic sequences (Ramaekers et al., 2007; Bosman and Ramaekers, 2015). Deposition of the mainly continental Athabasca Supergroup was accommodated by subsidence in three temporally discrete, but spatially overlapping, sub-basins (Ramaekers et al., 2007): the Jackfish, Cree, and Mirror sub-basins. The Jackfish sub-basin is a northeast-trending trough restricted to the westernmost Athabasca Basin that may have formed during crustal extension related to intrusion of the 1.77 to 1.73 Ga Kivalliq igneous suite in the hinterland of the Trans-Hudson Orogen (Bosman and Ramaekers, 2015),

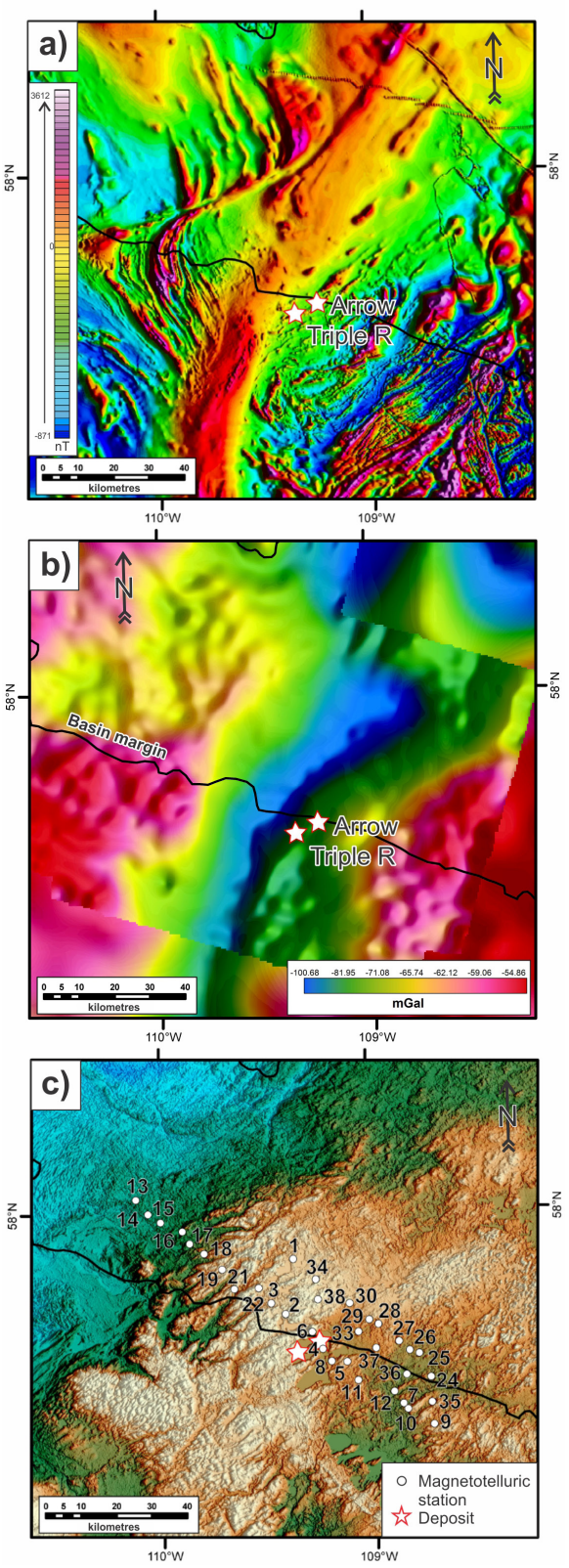

Figure 2. Geophysical data sets collected as part of the TGI uranium project over the southwestern Athabasca Basin: **a)** aeromagnetic residual total field grid; **b)** airborne Bouguer gravity grid displayed over the ground gravity grid; and **c)** magnetotelluric stations on the digital elevation model. (*After* Tschirhart et al., 2019)

overlapping with previous assessments of earliest deposition beginning at 1740 to 1730 Ma (Rainbird et al., 2007). The overlying Cree and Mirror sub-basins are elongate in an east-west direction, consistent with thermal subsidence (Rainbird et al., 2007; Ramaekers et al., 2007). Although the bulk of the Athabasca Supergroup was deposited in a continental environment, the presence of gypsum pseudomorphs and solution-collapse breccias in stromatolitic dolomite in the uppermost preserved formation (the Carswell Formation) suggests the development of marine evaporates (Hendry and Wheatley, 1985). Deposition of the underlying Douglas Formation shales at 1541 ± 13 Ma (Creaser and Stasiuk, 2007), constrained by whole-rock Re-Os geochronology, provides the youngest age constraint on preserved units of the basin, although deposition has been postulated to continue into the middle Mesoproterozoic based on correlations between the Hornby Bay, Thelon, and Athabasca basins (Rainbird and Young, 2009). As such, a minimum age for deposition of the Athabasca Supergroup is provided by the 1267 ± 2 Ma age of northwest-trending Mackenzie dykes (LeCheminant and Heaman, 1989), which crosscut all sequences in the Athabasca and Hornby Bay basins.

The Patterson Lake corridor and Athabasca Supergroup are unconformably overlain to the south by rocks of the Western Canada Sedimentary Basin. These comprise mixed siliciclastic and carbonate strata of the Lower to Middle Devonian Elk Point Group as well as sandstone, mudstone, and coal of the Lower Cretaceous Mannville Group (labelled 'Phanerozoic' in Fig. 1; Bosman et al., 2017). North of the study area, the 481.5 ± 0.8 Ma Carswell impact structure (Alwmark et al., 2017) exposes Paleoproterozoic crystalline basement rocks and overturned lower strata. The youngest deposits of the study area are unconsolidated glacial sediments deposited during multiple glaciations in the Quaternary. During the last glaciation in the Late Wisconsinan, the Laurentide Ice Sheet advanced and flowed generally southwestward over Saskatchewan from a dispersal centre in the Keewatin sector in Nunavut (Prest et al., 1968; Prest, 1984; Dyke and Prest, 1987; Dyke et al., 2002).

In the study area, the basement rocks of the Patterson Lake corridor comprise strongly foliated and metamorphosed granite, granodiorite, and mafic to ultramafic rocks and late, minor carbonatite dykes that are unmetamorphosed. The basement rocks lie within a subvertical, northeast-trending, heterogeneous, high-strain zone that is cut by a complex network of anastomosing brittle-ductile graphitic and chloritic shears and brittle faults. Uranium mineralization is localized within these subvertical shears and forms ore lenses that extend subvertically for up to 500 m (Card, 2017). The

Patterson Lake corridor records several hydrothermal–metasomatic events prior to primary uranium mineralization at ca. 1.4 Ga (Arrow deposit; Hillacre et al., 2019). These events caused widespread and pervasive silicification, extensive chlorite and sericite alteration, and finally late graphite and sulfide veining (Card and Noll, 2016; Card, 2017). Alteration minerals associated with uranium deposits in the Patterson Lake corridor include chlorite, muscovite, quartz (silicification), graphite, sulfide minerals (mainly pyrite, with lesser pyrrhotite, chalcopyrite, and galena), chlorite, illite, kaolinite, tourmaline, and hematite (Card and Noll, 2016; Cerin et al., 2017; Powell et al., 2019b). These mineral assemblages record multiple events in the corridor, including metamorphism (muscovite, chlorite, quartz flooding), pre-Athabasca Supergroup weathering (clays, iron oxides/hydroxide), magmatism (Clearwater Domain intrusions and carbonatite dykes), and hydrothermal mineralization (uraninite, hematite, illite, sudoite, tourmaline; Tschirhart et al., 2020).

GEOPHYSICAL INTERPRETATIONS

To refine the basement geology in areas of the Patterson Lake corridor and broader southwestern Athabasca Basin buried by sedimentary rocks and Quaternary cover, new airborne and ground geophysical data were acquired (Fig. 2): a high-resolution aeromagnetic survey (Natural Resources Canada, 2017), an airborne gravity survey (Natural Resources Canada, 2019), and two broadband magnetotelluric (MT) transects (Tschirhart et al., 2019). The new surveys were complemented by magnetic-susceptibility profiles for 27 drillholes (Tschirhart et al., 2020) and 92 physical property measurements for magnetic susceptibility, remanence, density, porosity, and resistivity. A suite of derivative products and edge enhancements were performed on the airborne geophysical data sets (Tschirhart et al., 2020) to enhance subtle variations in the physical-property responses, textural fabrics, and to accentuate long-wavelength sources. To highlight the long-wavelength response of geological domains and examine bulk physical property variations in the potential-field data, Tschirhart et al. (2020) generated a mosaic of the ground gravity data and upward continued aeromagnetic data. Before examining the district-scale geophysical expression of the Patterson Lake corridor, the geophysical analysis took a multi-step approach, whereby initial investigations were focused on the regional expression of geophysical and geological features, including differentiating the basement lithological units and interpreting the regional basin architecture (Tschirhart et al., 2020). This is being followed by more detailed investigations in the Patterson Lake corridor at the local scale (Tschirhart et al., 2020, work in progress).

The map area was subdivided into regional-scale geophysical domains using mosaicked Bouguer ground gravity anomalies, low-pass–filtered magnetic anomalies, and multi-scale edge analysis on the regional potential-field data sets. The domains were further classified by their magnetic and airborne gravity characteristics such as texture, amplitude, and orientation of anomalies, and validated by geological drillhole logs, where available, and magnetic susceptibility measurements (Fig. 3). Geological structures, such as faults, folds, and domain boundaries, were progressively incorporated from lineaments interpreted from lateral displacement of magnetic marker units (apparent strike-slip movement), abrupt reduction in anomaly wavelength (vertical displacement), linear demagnetized zones that crosscut the magnetic fabric, and topographic features.

The revised basement map by Tschirhart et al. (2020) identified new major features and refined the position and trend of previously proposed boundaries (Fig. 3). The spatial extents of structurally controlled buried felsic intrusions were interpreted and boundaries of the Taltson, Clearwater, and Tantato domains were redefined, including identifying a new buried basement domain containing dense, magnetic rocks located between the Harrison and Bustard faults and a new magnetic, low-density domain (ND on Fig. 3) similar in geophysical character to the Train Domain, located between the Grease River shear zone and the Black Bay fault. The potential field expression of the new domain may be due to an abundance of low-density, magnetic Hudson suite granites and/or metasomatism, as is the case in the Train Domain (Ashton et al., 2018). With respect to the architecture of the basin, the regional geophysical analysis identified several new features, including an interpreted major structural break that is recorded in Athabasca Basin isopach maps where the northwestern hanging wall (Taltson) is down-dropped relative to the southeastern footwall (Tantato), indicating post-depositional movements (Fig. 1, DL on Fig 3). The timing and movement of this fault correlates with accommodation space that localized the early Jackfish sub-basin (Ramaekers et al., 2017). Another northeast-trending, crustal-scale structure was interpreted separating the southern Tantato Domain from the Taltson Domain (Fig. 3), terminating at the Clearwater Domain and variably intruded to the northeast by as yet unsampled voluminous felsic intrusions (Int1, Int2, Int3 on Fig. 3).

The MT data provide information on the resistivity (and conductivity) of the subsurface and the gravity data provide information on the subsurface density distribution. Strike and phase tensor analysis of the MT data identified predominantly 3-D geometries (McNeice

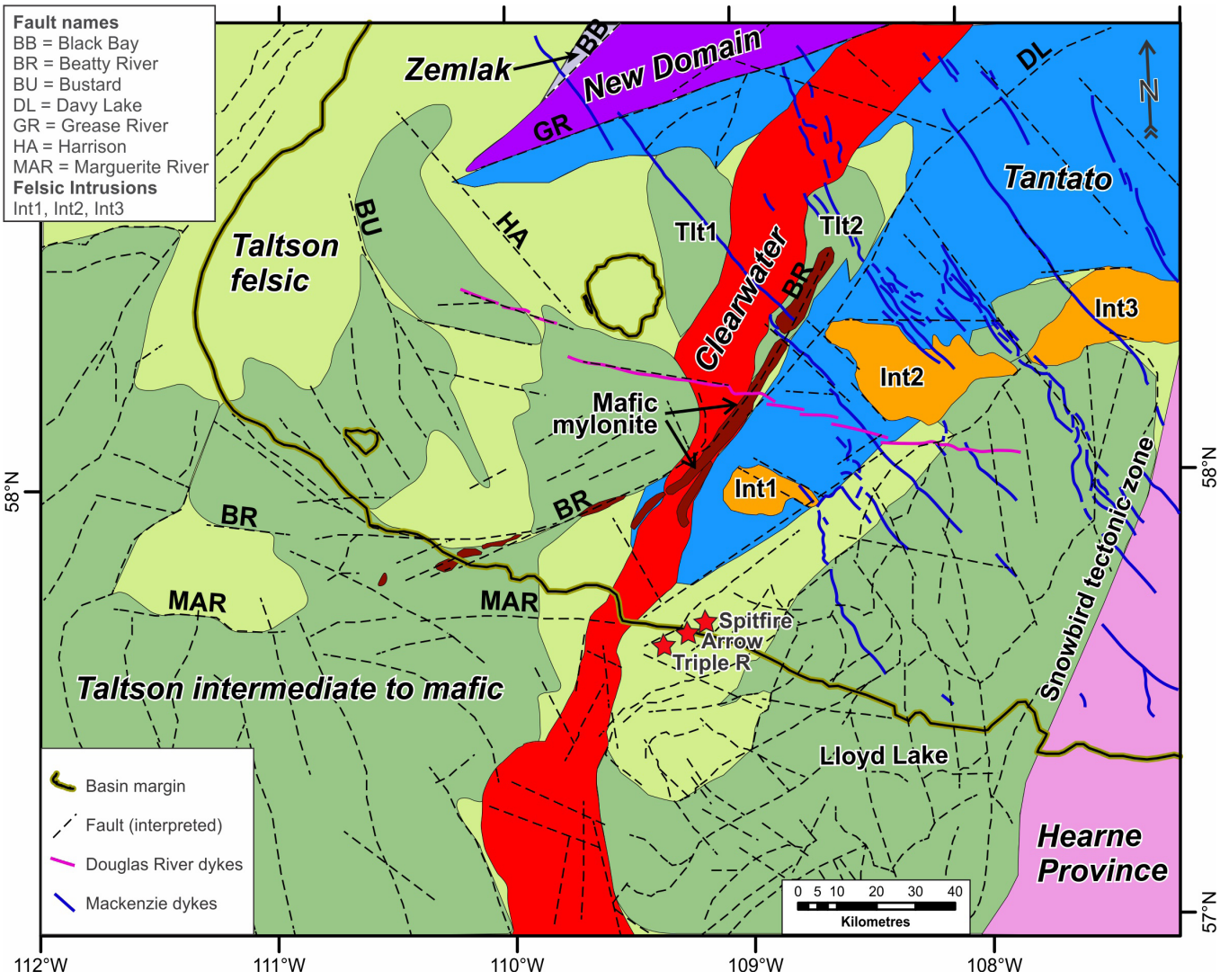

Figure 3. Geophysical-geological domains and basement structures of the southwestern Athabasca Basin (dark brown line), determined by magnetic and airborne-gravity characteristics and validated by drill-core magnetic-susceptibility measurements where available (*after* Tschirhart et al., 2020).

and Jones, 2001; Caldwell et al., 2004); however, when the 2-D inversion (Fig. 4) was interpreted alongside preliminary 3-D MT and gravity inversions, robust features emerged (Tschirhart et al., 2019). Below the Arrow deposit, a conductive corridor was imaged that extends to the mantle (Fig. 4). Sensitivity testing of the 2-D inversion requires the feature be present in that model for the 2-D response of selected 2-D periods (Tschirhart et al., 2019) — its removal results in a 10% increase in the root mean square error. The presence of the conductivity anomaly on the 3-D inversions is consistent with a robust feature and adds insight into the role of deep-seated fluid corridors in the location of ore deposits. Near-surface conductors are located over graphitic fault zones and mapped zones of conductive Phanerozoic cover (Tschirhart et al., 2019). North of the Beatty River shear zone, underneath the Athabasca Basin, conductive bodies were imaged approximately 10 to 30 km below surface. These bodies may correspond with fold-thickened, sulfide-bearing rocks such as the Rutledge River complex, which occurs along trend north of the basin (e.g. Rukhlov, 2011). The Clearwater Domain is notable as a high-resistivity, low-density feature that extends to the mantle and is located below the Patterson Lake corridor at depth (Tschirhart et al., 2019). A low-density anomaly is similarly modelled extending to the Mohorovičić discontinuity using the gravity data (Potter et al., 2019).

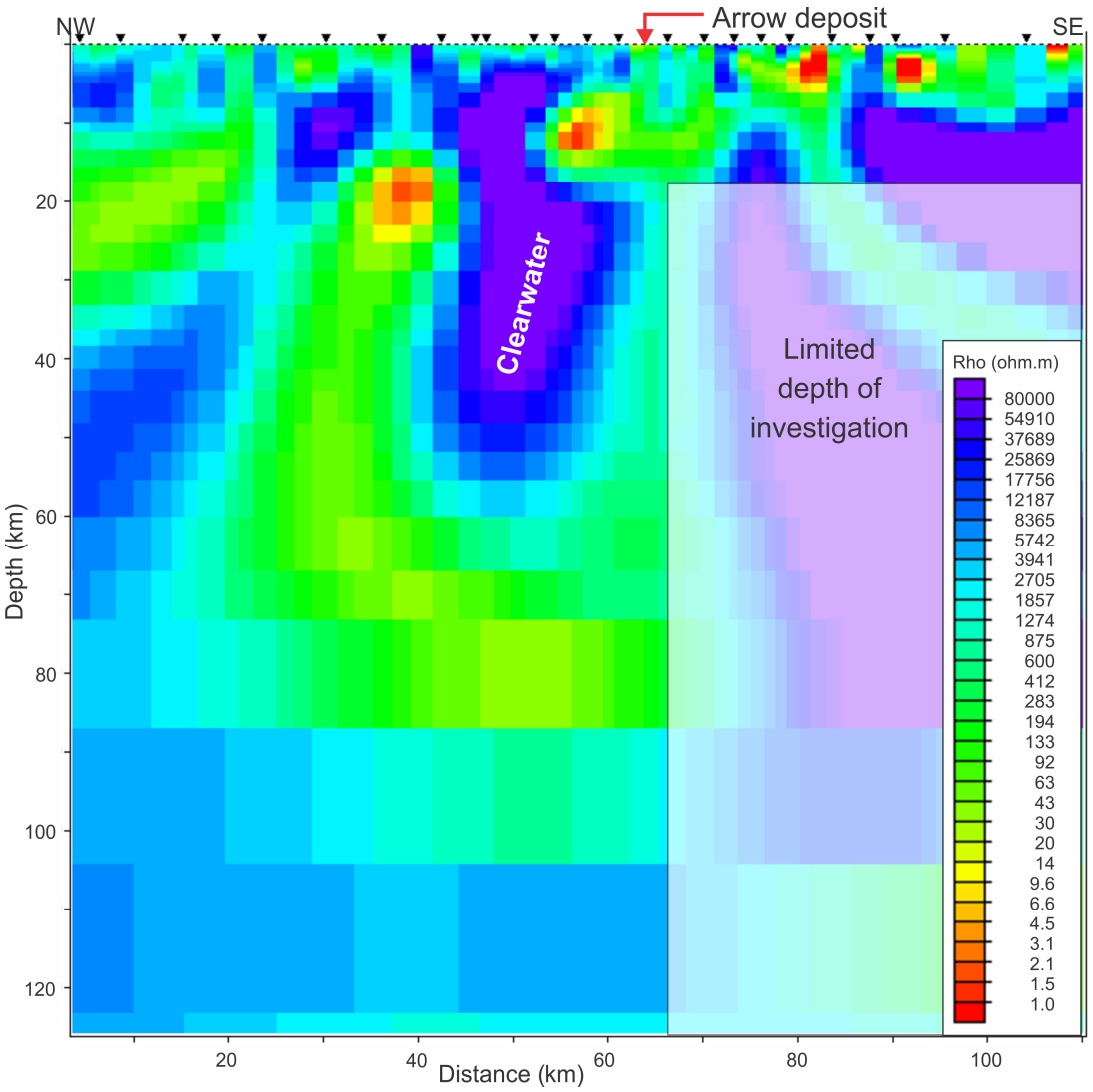

Figure 4. Two-dimensional inversion of the magnetotelluric data for the transect over the Arrow deposit at select 2-D periods to 5.7 s. Root mean square error = 2.53 (for error floors ρaTE = 20%, ΦTE = 10%, ρaTM = 10%, and ΦTM = 5%). McNeice and Jones (2001) strike direction (multisite, multifrequency) is 24°, *after* Tschirhart et al. (2019, work in progress).

BASEMENT GEOLOGY – THE CLEARWATER DOMAIN

As noted above, the Clearwater Domain is one of the most prominent geophysical features in northern Saskatchewan, forming a curvilinear aeromagnetic high and gravity low that effectively divides the Taltson Domain into eastern and western segments while truncating the southern limit of the Patterson Lake corridor (Fig. 1, 3). Covered by the Proterozoic Athabasca Basin and younger Cretaceous and Devonian sedimentary rocks, only one outcrop of the domain has been discovered, south of the project area along the Clearwater River (Sibbald, 1974; Stern et al., 2003). In drill core, the Clearwater Domain rocks are predominantly plutonic and typically consist of weakly foliated, post-metamorphic granitic bodies intruding older granitic gneiss (this study; Card, 2018). Sampling from three industry drillholes (Fig. 5) above the Clearwater geophysical anomaly revealed variably deformed, biotite-bearing, peraluminous granitic rocks. Crosscutting relationships indicate several phases of intrusion, plus a generation of late granitic pegmatite and aplitic dykes. Using concentrations of K, Th, and U, the radiogenic heat production (RHP; in μWm^{-3}) was calculated using Rybach (1988):

$$RHP\ (\mu Wm^{-3}) = \rho(9.67C_U + 2.56C_{Th} + 2.89C_{K_2O}) \times 10^{-5} \quad (1)$$

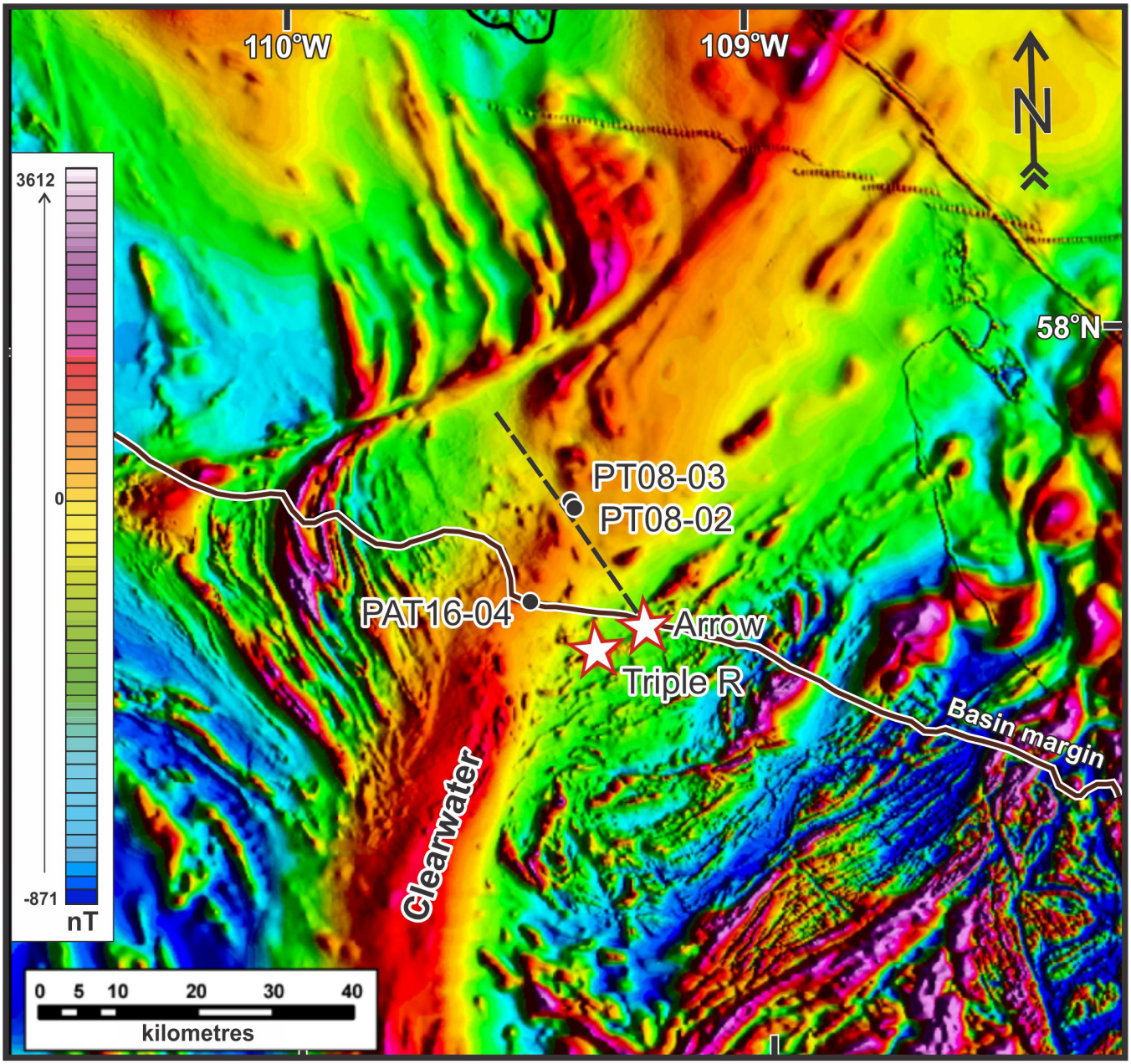

Figure 5. Location of the industry drillholes intersecting Clearwater Domain granites sampled in this study, northwest of the Patterson Lake corridor deposits (stars), overlain by the residual total field aeromagnetic survey (Natural Resources Canada, 2017). The PT08-series drillholes are situated above a structural break (dashed line) in the magnetic anomaly that trends southeast to the Arrow deposit.

where C is the concentration of heat-producing elements in parts per million (U, Th) and weight per cent (K_2O), and ρ is the density in kgm^{-3}. Using this relationship, the RHP of the Clearwater samples ranged from 1.19 to 6.14 μWm^{-3} (mean = 3.86 μWm^{-3}; Fig. 6), which is elevated compared to mean values for granite (3.46 μWm^{-3}), granodiorite (1.84 μWm^{-3}; a proxy for the host dioritic gneisses), and upper continental crust (approximately 1.6 μWm^{-3}; Jaupert et al., 2016; Hasterok et al., 2018). This range excludes an altered fault-zone sample, which yielded a value of 14.49 μWm^{-3} due to elevated uranium content (44 ppm U, 37.4 ppm Th). Analysis of a sample from the only known outcrop of Clearwater Domain granite, approximately 100 km south of the study area, yielded higher uranium contents and RHP (7.13 μWm^{-3} using data from Card, 2002; Fig. 6).

Despite forming a magnetic high, magnetic susceptibilities measured on drill core above the Clearwater Domain anomaly were nonmagnetic (0.00030 SI;

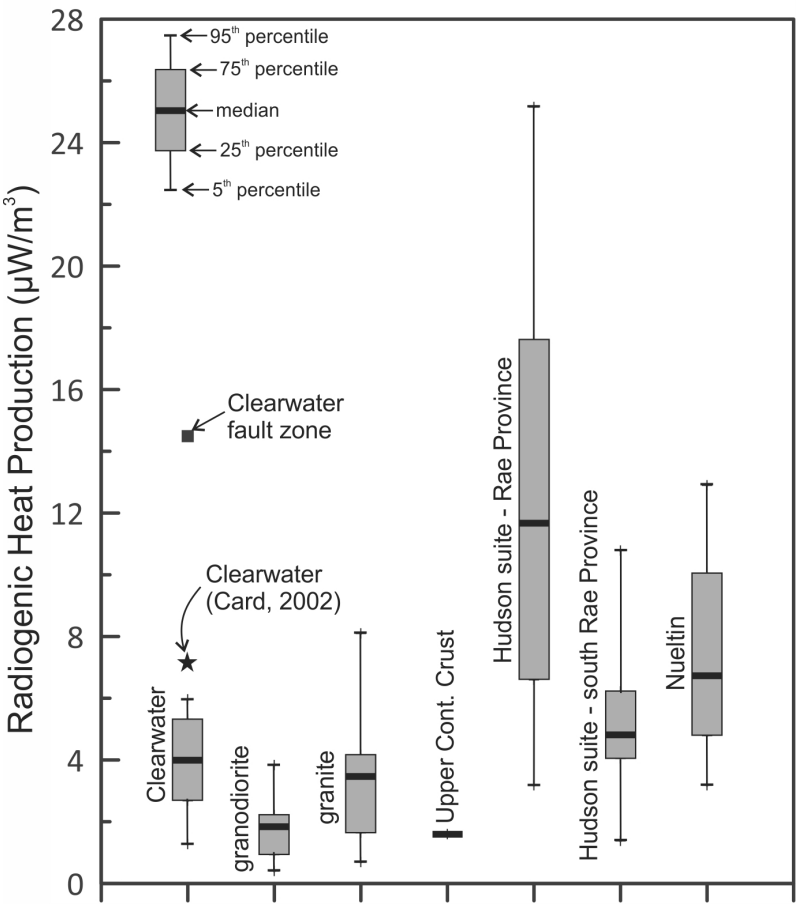

Figure 6. Radiogenic heat production of the Clearwater Domain samples compared to values for granodiorite and granite (Hasterok et al., 2018), upper continental crust (Jaupert et al., 2016), and Hudson and Nueltin granitic suites (calculated from data in Peterson et al., 2002, in press; Scott et al., 2015). Radiogenic heat production calculated using Rybach (1988).

Tschirhart et al., 2020). The granitic samples analyzed are also peraluminous and plot within the 'A-type' granite field of Whalen et al. (1987), in contrast to the magnetic signature. Together, these data suggest that the magnetic anomaly lies at depth, possibly reflecting multiple intrusive phases related to partial melting of metasedimentary rocks or granulite-facies residues (Whalen et al., 1987). Field observations from the only known outcrop of Clearwater granite also revealed several phases of Clearwater intrusions. Card (2002) noted that the contacts between the various intrusive phases, rims of gneissic xenoliths, and late aplitic dykes are magnetic, suggesting that the aeromagnetic high is underlain by a complex, multi-phase intrusion in which magnetite formed along contacts between intrusive phases and xenoliths.

In drillhole PT08-002, brittle deformation and hydrothermal alteration of the Clearwater Domain granite resulted in the formation of a breccia zone (approximately 10 m wide from 331–341 m) with elevated U, heavy rare-earth elements, Cu, Co, Cr, Pb, Mg, and Fe^{3+} and depleted Fe^{2+}, Ca, Na, Sr, and light rare-earth-element contents relative to the average of six samples of least-altered granite from the same drillhole (Fig. 7). Visible in the regional aeromagnetic data (Fig. 2a, 3, 5), this structure causes a break in the Clearwater magnetic anomaly and trends southeast toward the Arrow deposit. In the same drillhole, Athabasca Supergroup pebbly sandstone directly overlies a weathered Clearwater Domain granite. The unconformable contact preserves a hematitic horizon that transitions into chloritized then relatively fresh granite (i.e. the Athabasca red-green zone of MacDonald [1985]). The horizon records significant depletion in most elements (e.g. Fe^{2+}, Mn, Mg, Ca, Na, K, Rb, Cs, Ca, rare-earth elements [REE], U), and weak enrichment in Al, Fe^{3+}, and Ta. The lower uranium, contents, lower RHP, brittle fault zone enriched in uranium, and petrography support leaching of uranium from the Clearwater Domain granites in the vicinity of the deposits (Potter et al., work in progress).

Stern et al. (2003) reported a U-Pb zircon age of 1843 ± 4 Ma for the Clearwater Domain from the only known exposure along the Clearwater River, linking the intrusions to a suite of monzogranite plutons emplaced between 1830 ± 25 Ma (Stern et al., 2003) and 1819 ± 28 Ma (Bickford et al., 1994). New zircon U-Pb dating was conducted on three samples of the peraluminous granitic rocks from two drillholes above

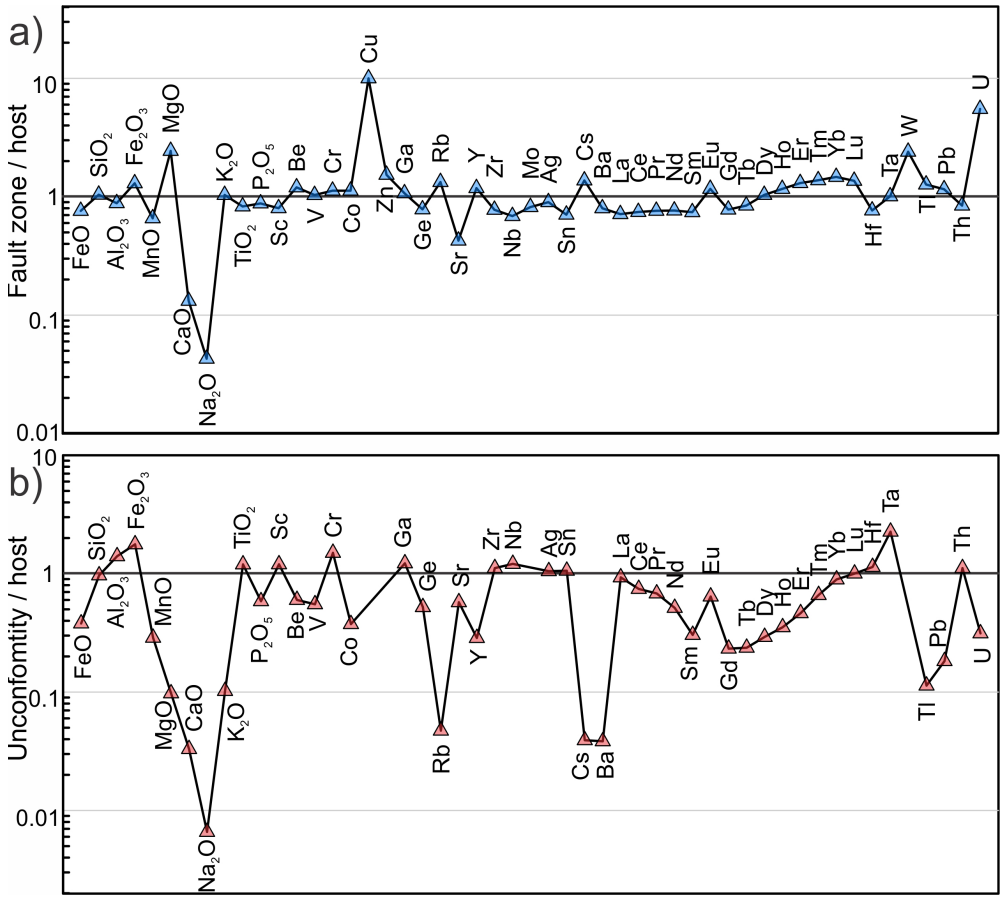

Figure 7. Element enrichment and depletion patterns of the **a)** shear zone, and **b)** unconformity contact within Clearwater granite intrusions intersected in drillhole PT08-002, normalized to six samples of the least-altered Clearwater intrusion hosting the shear zone and below the unconformity.

the Clearwater Domain aeromagnetic high. Samples were selected from crosscutting phases of the intrusion. Following mineral separation, zircon grains were mounted in epoxy and analyzed using the sensitive high-resolution ion microprobe (SHRIMP II) at the Geological Survey of Canada (Ottawa, Ontario). Analyses followed the procedures outlined in Stern (1997) and Stern and Amelin (2003). Most zircon grains in each sample were highly altered, but subpopulations of magmatic zircon were recognized based on their prismatic shape and characteristic oscillatory zoning. Preliminary interpretations of the results yielded weighted mean $^{207}Pb/^{206}Pb$ ages that overlap in error with the published ages of 1843 ± 4 Ma (Stern et al., 2003; Powell et al., 2019a). Inherited zircon grains include a population of concordant ca. 1.9 Ga zircon grains that correspond to the age of regional high-pressure metamorphism (Powell et al., 2018a), and 2.2 to 2.8 Ga zircon grains consistent with the Taltson basement complex (McNicoll et al., 2000). To the southwest, along the southern margin of the Snowbird tectonic zone, the Rimbey Arc consists of biotite granitoids that are correlative in age (ca. 1.79–1.85 Ga; e.g. Ross, 2002) and exhibit a similar linear magnetic anomaly to the Clearwater Domain. If the Clearwater Domain and Rimbey Arc represent offset segments of the same 1.80 to 1.85 Ga magmatic belt emplaced during a continental extensional event (Card, 2018), then dextral movements along the Snowbird tectonic zone may have reached at least 150 km; further studies are required.

STRUCTURAL HISTORY

Studies led by Johnstone et al. (2019) indicate that the structural architecture of basement rocks in the Patterson Lake corridor is primarily the result of complex type-2 transitional to type-3 fold interference, whereby a strong gneissosity (S1/S2) related to northwest-trending ‘hook’ fold patterns is transposed to the northeast to create a

regional type-3 ‘boomerang’ fold interference pattern (F3). In the Patterson Lake corridor, which is located in the northeast limb of the regional F3 fold, S1/S2 is transposed and overprinted by a near-vertical, east-southeast–dipping, axial-planar spaced cleavage associated with the regional F3 fold pattern. This geometry has been interpreted from macroscopic-scale curvilinear magnetic-map patterns, as well as mesoscopic-scale fold-interference patterns in drill core (Fig. 8). These complex fold-interference patterns likely developed during transposition of northwest-trending 1.94 to 1.93 Ga Taltson fabrics by northeast-trending 1.92 to 1.90 Ga Snowbird fabrics. In addition, the regional-scale buckle fold, which is cored along its axial trace by the Clearwater Domain, developed during transposition that took place 1.92 to 1.90 Ga during the Snowbird Orogen. Subsequent reverse oblique right-lateral ductile shearing (D4) resulted in additional shortening, steepening, and lateral transposition of earlier Taltson-Snowbird fabrics along the Patterson Lake corridor’s main northeast trend. This event is thought to coincide with other northeast-trending transpressional shearing events (e.g. Beatty River shear zone) and associated antithetic north-northwest–trending sinistral shears that are present throughout the region (Fig. 3). Northeast-trending ductile shears in the Patterson Lake corridor were subsequently reworked and transposed by brittle-ductile deformation (D5). This event is marked by the development of superimposed east-northeast–trending, steeply southeast-dipping, oblique reverse dextral graphitic-chloritic shears, which form an anastomosing network of conductors that host uranium mineralization. Figure 9 displays an interpretation of the D4/D5 shearing system that is present throughout

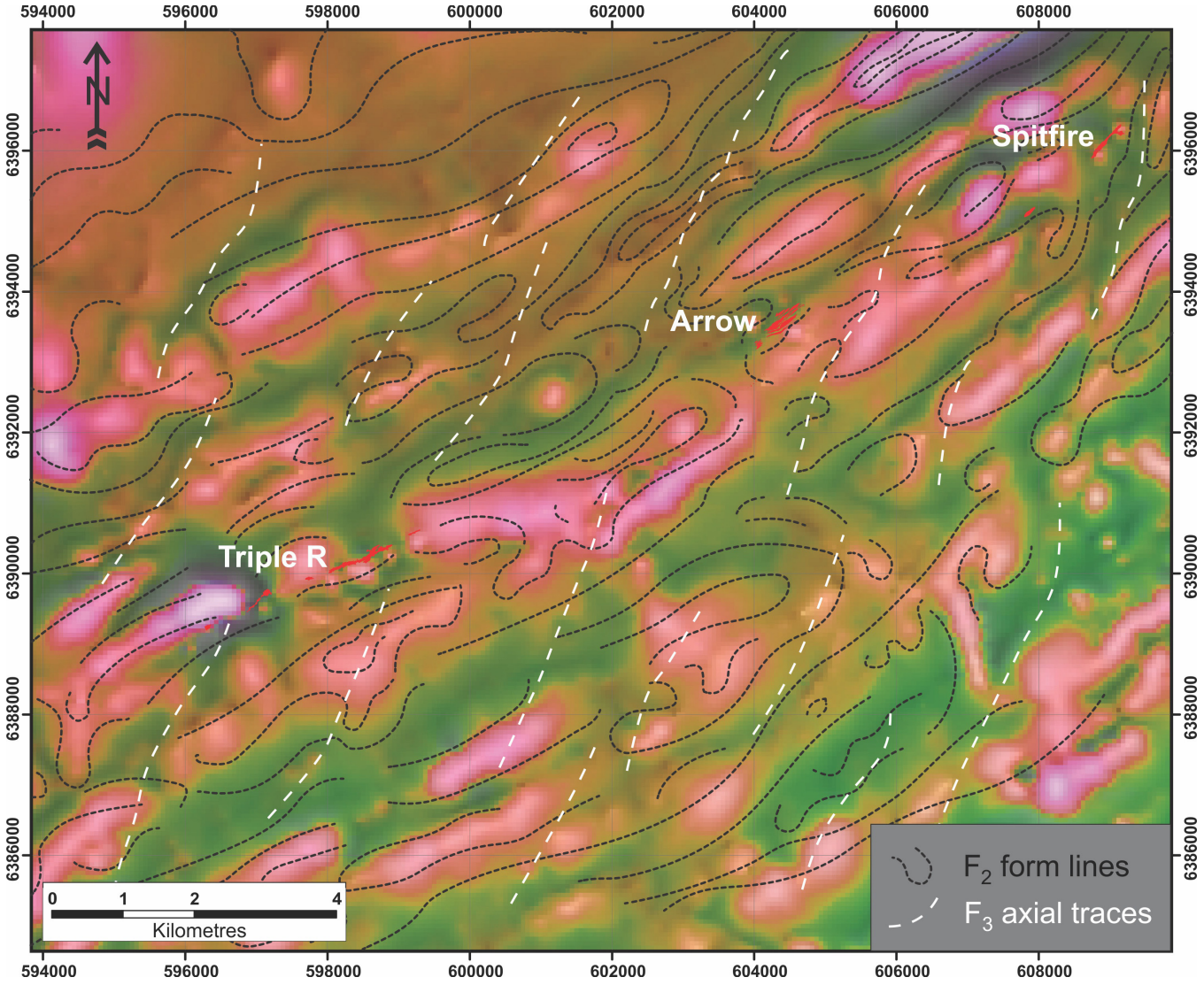

Figure 8. Natural Resources Canada (2017) total-residual-field and tilt-angle magnetic maps (overlain with 35% transparency), and interpreted early fold-interference patterns near the Triple R, Arrow, and Spitfire deposits (Johnstone et al., 2019).

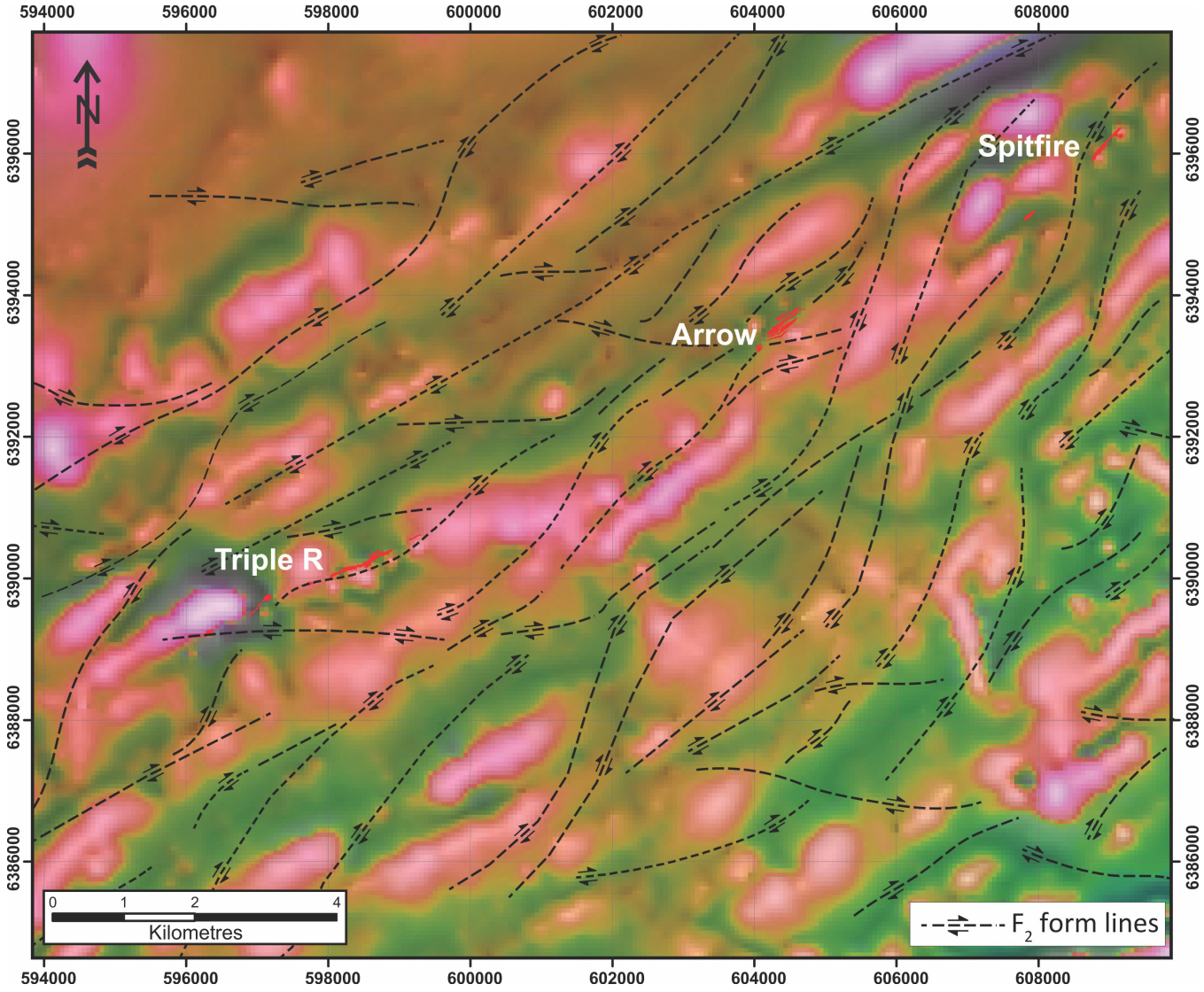

Figure 9. Natural Resources Canada (2017) total-residual-field and tilt-angle magnetic maps (overlain with 35% transparency), and the interpreted brittle-ductile, C-S type structural style present throughout the Patterson Lake corridor (Johnstone et al., 2019).

the Patterson Lake corridor. The complex organization of these structures is the result of strain partitioning across basement units of contrasting rheology (extensive silicified zones versus the various gneisses) and the pre-existing ductile structural grain.

The development of the Athabasca Basin is thought to be associated with east- and northeast-trending transtensional shears (Ramaekers et al., 2017) and related north-trending normal faults that cut all basement rocks and have migrated into the overlying Athabasca sandstones (Fig. 10). West- and west-northwest–trending conjugate faults and centimetre-scale subhorizontal reverse faults cut the Athabasca Supergroup and are thought to be responsible for oblique reverse reactivation of the brittle-ductile (graphitic-chloritic) shears (Fig. 11). In addition, southeast-striking sinistral faults result in vertical left-stepping dilatational jogs along the early northeast-trending, semi-ductile structural grain. These crosscutting faults most likely provided pathways for uranium-bearing fluids to move through and penetrate along the reactivated brittle-ductile structural grain.

As part of the TGI project, Ma et al. (2019) noted similar relationships in the Bathurst fault zone, located north of the project area in the eastern Slave Craton. This fault zone, which trends north-northwest–south-southeast, displaced the ca. 1.9 Ga Kilohigok Basin and the 2.07 to 1.96 Ga Thelon tectonic zone and intersects the 1.7 Ga Thelon Basin, where basement faults host uranium occurrences (e.g. Miller et al., 1984; Fuchs et al., 1986; Fuchs and Hilger, 1989). Ma et al. (2019)

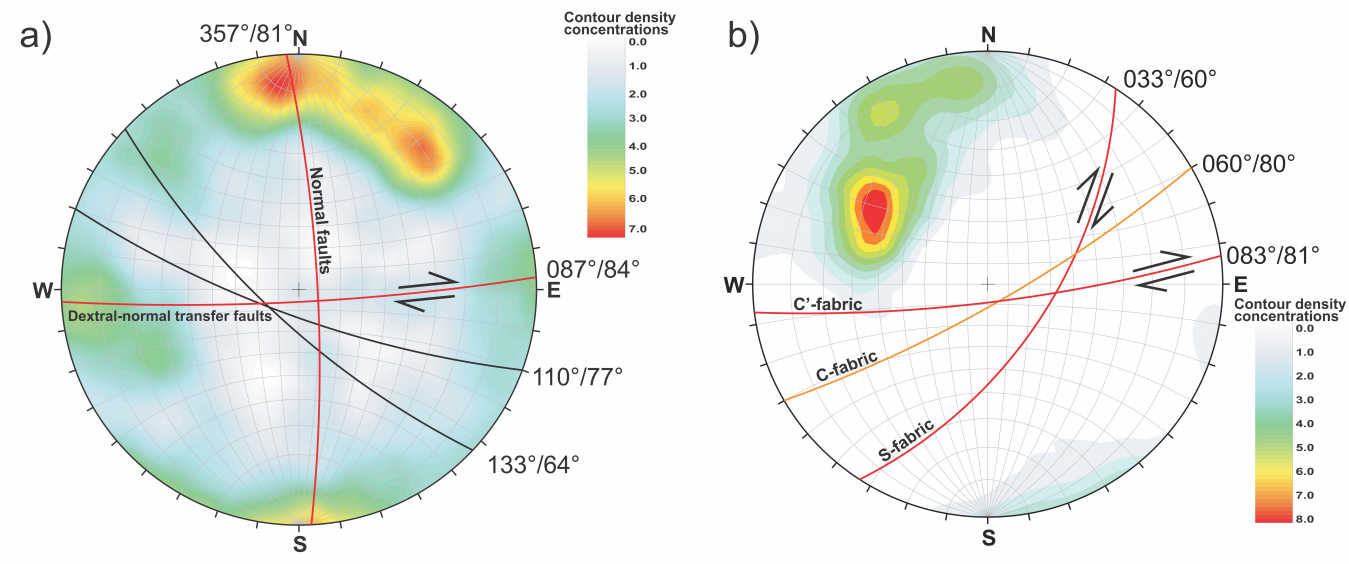

Figure 10. Equal-area stereonet projections of **a)** all sandstone structures and **b)** the reactivation of brittle-ductile shears in basement rocks of the Patterson Lake corridor (Johnstone et al., 2019).

reported that ductile flattening fabric developed between ca. 1933 and 1895 Ma and was associated with the orthogonal collision and indentation of the Slave Craton into the Thelon tectonic zone and Rae Province. Brittle deformation was localized parallel to the ductile flattening fabric after ca. 1840 Ma and enhanced fluid permeability along the fault.

FLUID INCLUSION STUDIES

Drill-core logging and petrographic studies from several locations in the Patterson Lake corridor revealed multiple generations of quartz veining (Fig. 12; Cerin et al., 2017; Rabiei et al., 2018, 2019, work in progress). White metamorphic quartz (Q1), blue quartz (Q2), blue-milky quartz (Q3), smoky quartz (Q4), and basin syntaxial quartz (Q5) formed prior to uranium mineralization, whereas drusy quartz in the Athabasca sandstones (Q6) and basement rocks (Q7) crystallized during or post-mineralization, based on coexistence with white mica, chlorite, and tourmaline generations associated with uranium mineralization. Quartz veins and breccia paragenetically associated with uranium mineralization are characterized by elevated radiation-induced defects (Cerin et al., 2017) and contain uranium-rich fluid inclusions (Rabiei et al., 2019), supporting the interpretation of quartz precipitation during or after the main mineralization event. This relationship has been documented in deposits throughout the Athabasca Basin, where quartz-forming fluids (i.e. NaCl-rich and $CaCl_2$-rich brines) equilibrated with illite, sudoite, and dravite with respect to oxygen isotopes (Richard et al., 2013) and quartz crystals contain fluid inclusions with high concentrations of uranium (Richard et al., 2010, 2012, 2016). Analysis of primary fluid inclusions hosted in pre-ore Q3 and Q4 yielded salinities ranging from 0.2 to 4.5 weight per cent NaCl, with X_{NaCl} values ($NaCl/(NaCl + CaCl_2)$) equal to 1. Fluid inclusions within syn- to post-ore Q6 and Q7 yielded salinities ranging from 24 to 26 weight per cent $NaCl + CaCl_2$ and X_{NaCl} values ranging from 0.3 to 0.7 (Fig. 13). These results indicate that brine salinity increased following

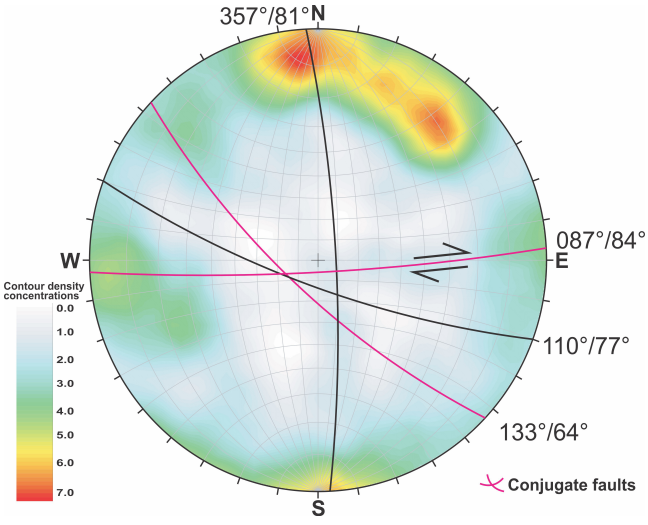

Figure 11. Equal-area stereonet projecting all sandstone structures with superimposed interpretation of late-phase conjugate faults in the Patterson Lake corridor (Johnstone et al., 2019).

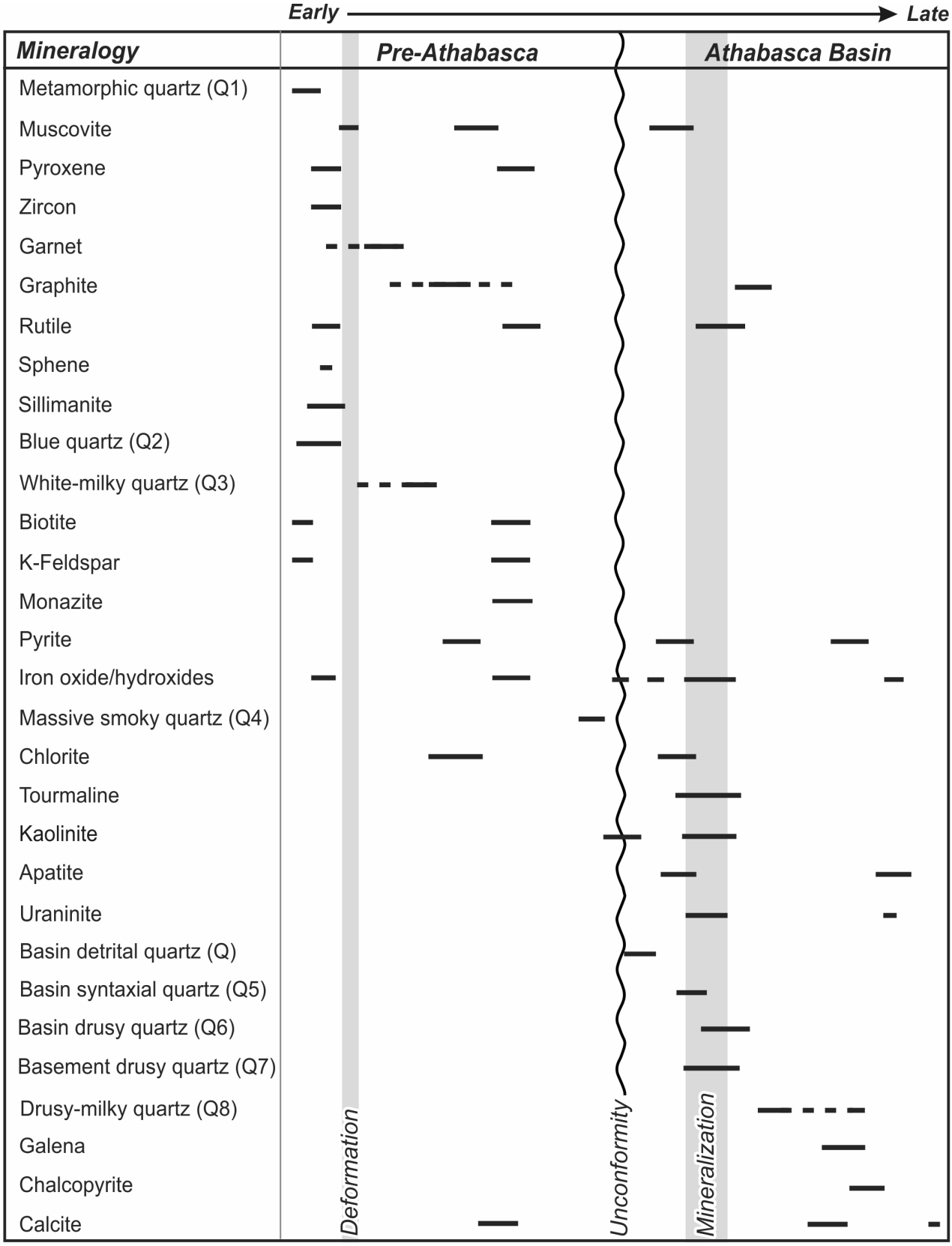

Figure 12. Generalized paragenetic sequence of the Patterson Lake corridor (Rabiei et al., 2019).

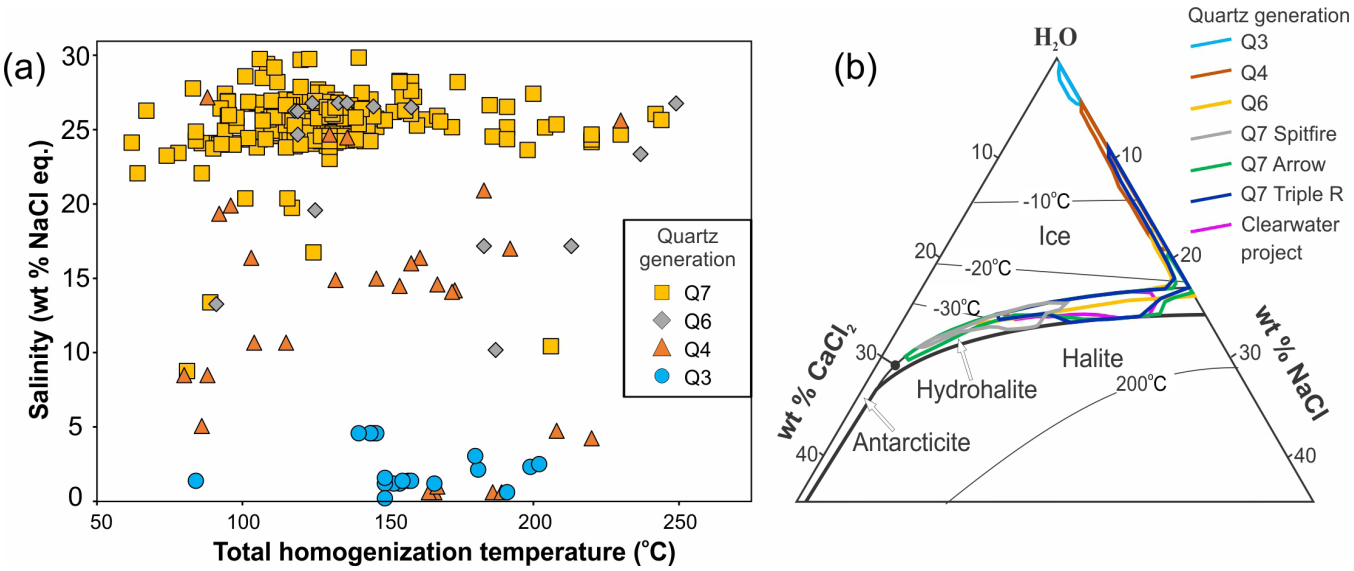

Figure 13. a) Total homogenization temperature versus salinity and **b)** H_2O-NaCl-$CaCl_2$ phase diagram for fluid inclusions within the different generations of quartz veins (Rabiei et al., 2019).

deposition of the Athabasca Basin, as recorded in syn-mineralization quartz veins from the basement and basin. Fluid inclusions in Q6 and Q7 also trapped both NaCl- and $CaCl_2$-brines along the known vertical and lateral extent of the Patterson Lake corridor, with no systematic variation in salinity or Ca-Na ratio relative to depth. Total homogenization temperatures of primary, pseudosecondary, and secondary fluid inclusions in Q6 and Q7 range from 83 to 215°C (Fig. 13a), similar to ranges reported from the eastern basin (e.g. Poty and Pagel, 1988; Kotzer and Kyser, 1995; Derome et al., 2005), and do not show significant temporal or spatial variations. Derome et al. (2005) proposed the range in homogenization temperatures records fluid mixing between warmer NaCl-rich basin brines and cooler $CaCl_2$-rich brines that formed through interactions between the NaCl-rich brines and basement rocks. Chi et al. (2019), however, documented the development of Ca-rich uraniniferous diagenetic fluids within the basin. The formation of $CaCl_2$-rich brines through Ca-Na exchange with the Ca-bearing minerals in the basement rocks should also cause extensive sodic alteration. Although Hoeve and Sibbald (1978) reported 'plagioclasite' basement rocks at the Rabbit Lake deposit, they appear to be disconnected to brine circulation (Richard et al., 2013) and widespread albitization of basement plagioclase has not been observed (Alexandre et al., 2005; Mercadier et al., 2010). The coexistence of liquid-dominated, vapour-dominated, and vapour-only fluid inclusions in fluid inclusion assemblages (Fig. 14) from barren and mineralized zones suggests fluid boiling during mineralization, a feature that has also been proposed for uranium deposits in the eastern part of the Athabasca Basin (Chi et al., 2014, 2018; Wang et al., 2018). Under normal geothermal gradients, a fluid with 25 weight per cent NaCl cannot boil at the temperatures indicated by the fluid inclusion data. The only mechanism to explain the boiling is by faulting, which causes rapid changes in pressure (Chi et al., 2014, 2017; Wang et al., 2018; Rabiei et al., 2019, work in progress).

ISOTOPIC EXPRESSIONS OF THE SYSTEMS

The protracted fluid-rock interactions documented along the Patterson Lake corridor (e.g. Card, 2017, 2018; Johnstone et al., 2019; Rabiei et al., 2019) have resulted in the mobilization, transportation, and precipitation of multiple generations of alteration minerals, amplifying stable-isotope fractionations. One possible mechanism for the precipitation of uranium is coupled reduction-oxidation (redox) reactions between iron-bearing basement minerals and uranium-bearing oxidized brines (Bray et al., 1982). In Mount (2019), iron isotopes in pyrite were used to unravel the fluid history and nature of uranium deposition in the Patterson Lake corridor. Iron isotopes are strongly fractionated during redox reactions (Johnson et al., 2008), which can result in enrichment in heavier ^{56}Fe and ^{57}Fe isotopes associated with uranium ore bodies (Acevedo and Kyser, 2015; Potter et al., 2015, work in progress). Given the abundance of sulfide minerals (dominantly pyrite) in the metamorphosed mafic

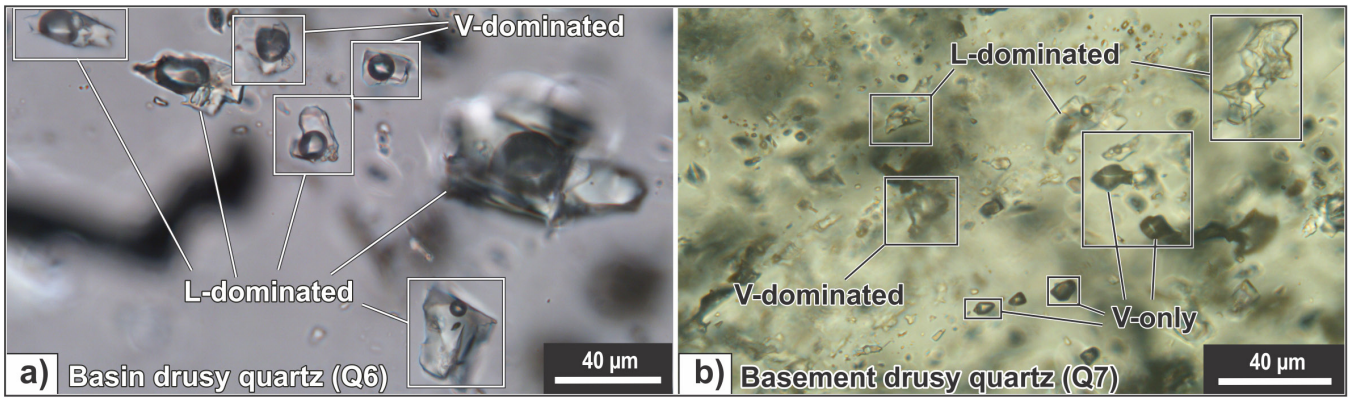

Figure 14. Fluid inclusions with different vapour ratios from drusy quartz veins synchronous with mineralization in the **a)** basin and **b)** basement (812.9 m depth) in the Athabasca Basin (*after* Rabiei et al., 2019).

basement rocks of the Patterson Lake corridor, reduction of sulfide minerals in the ore zone, and association of hematite with the ore zones (Fig. 15), one mechanism to precipitate the ore is the reaction between pyrite and oxidized, uranium-bearing fluids (Scott et al., 2007):

$$2FeS_2 + UO_{2\,[aq]}^{2+} + 2H_2O + 7O_2 \rightarrow 2Fe^{3+} + 4SO_4^{2-} + UO_{2[s]} + 4H^+ \quad (2)$$

Iron isotopic values are reported in delta notation ($\delta^{56}Fe$) in per mil (‰) relative to isotopic reference material (IRMM-014; Taylor et al., 1992):

$$\delta^{56}Fe = \left(\frac{^{56}Fe/^{54}Fe_{sample}}{^{56}Fe/^{54}Fe_{standard} - 1} \right) \times 10^3 \quad (3)$$

As reported in Mount (2019), in-situ laser-ablation inductively coupled plasma mass spectrometry (LA-ICP-MS) analysis at the Geological Survey of Canada (Ottawa, Ontario) and secondary-ion mass spectrometry (SIMS) at the University of Manitoba (Winnipeg, Manitoba) produced some of the largest documented variations in $\delta^{56}Fe$ values of hydrothermal pyrite, ranging from approximately –1.3 to +1.67‰ at the Triple R deposit (Fig. 16). Isotope values varied with depth, within individual samples, and even within single pyrite grains. For example, the $\delta^{56}Fe$ values in a single pyrite grain sampled from drill core PLS14-177 at 268 m depth yielded values of 0.31 to 1.67‰ (Fig. 16b). These isotopic values stray from reported whole-rock values of mafic to ultramafic rocks expected from pyrite in the basement rocks (–0.1 to +0.2‰, including errors; Craddock and Dauphas, 2010). This implies that the original iron isotopic compositions of the primary magmatic sulfide minerals in the underlying mafic to ultramafic units of the Patterson Lake corridor were repeatedly fractionated during fluid-rock interactions to induce such large fractionations. As noted by Polyakov and Soultanov (2011), pyrite is often enriched in light iron isotopes (e.g. ^{54}Fe) in hydrothermal or sedimentary environments (e.g. Beard and Johnson, 2004; Rouxel et al., 2004, 2008; Johnson et al., 2008). This enrichment is also documented at mid-oceanic ridges, where leaching of iron from basalt typically results in the preferential release of the lighter iron isotopes (Rouxel et al., 2003). In contrast, as shown in Figure 16, pyrite grains below and within the ore zones are generally enriched in heavier iron isotopes, generating positive $\delta^{56}Fe$ values. Previous studies have shown that iron oxidation can generate significant enrichment in heavier iron isotopes (Severmann et al., 2004; Johnson et al., 2008). Furthermore, the significant variation in iron-isotope values within single pyrite grains and individual samples suggests that the pyrite grains likely underwent multiple generations of dissolution by oxidation, precipitation of oxidized products, sulfidization, and eventual oxidation during hydrothermal fluid alteration. In drill core, sulfide minerals are reduced in abundance and grain size in the ore zones, and the ore zones are broadly associated with hematite halos, supporting the recycling of iron and sulfur.

As documented in other Athabasca Basin deposits (e.g. Rosenberg and Foit, 2006; Mercadier et al., 2012; Adlakha et al., 2017), magnesium-rich hydrothermal tourmaline occurs in the alteration halo of the Patterson Lake corridor deposits. Tourmaline contains boron, a fluid-mobile, moderately volatile lithophile element that has two stable isotopes: ^{10}B and ^{11}B (Bast et al., 2014). The boron isotopic composition is reported in delta notation ($\delta^{11}B$) as the per mil (‰) deviation of the instrumental mass fractionation (IMF) corrected isotopic ratio ($R_{Corr} = IMF \times R_{Meas}$, where R_{Meas} = measured isotopic ratio) from the SRM 951 boric acid reference value ($R_{SRM951} = 4.04362$; cf. Marschall and Foster, 2018):

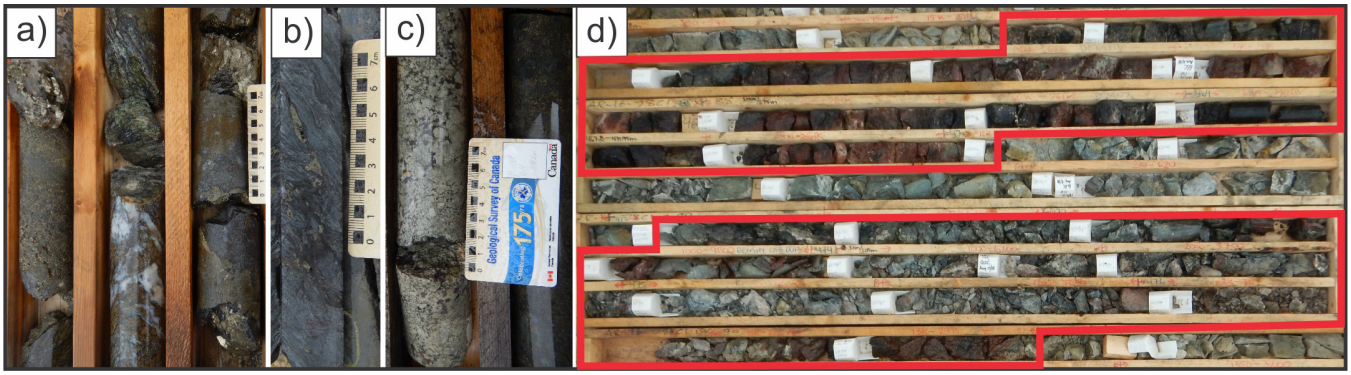

Figure 15. Photographs of drill core from deposits in the Patterson Lake corridor. **a)** Pyrite-rich, intensely silicified and altered orthogneiss below the ore zones at the Triple R deposit. NRCan Photo 2019-785 **b)** Graphite- and sulfide-rich shear zone with open-space textures below the Spitfire. NRCan Photo 2019-786 **c)** Altered pyroxenite-ultramafic units with disseminated sulfide minerals and graphite from the basement to the Triple R. NRCan Photo 2019-784 **d)** Sulfide-poor, hematite-rich zones straddling within mineralized (red boxes) graphitic shear zone, Arrow deposit. NRCan Photo 2019-787 (All photographs by E.G. Potter)

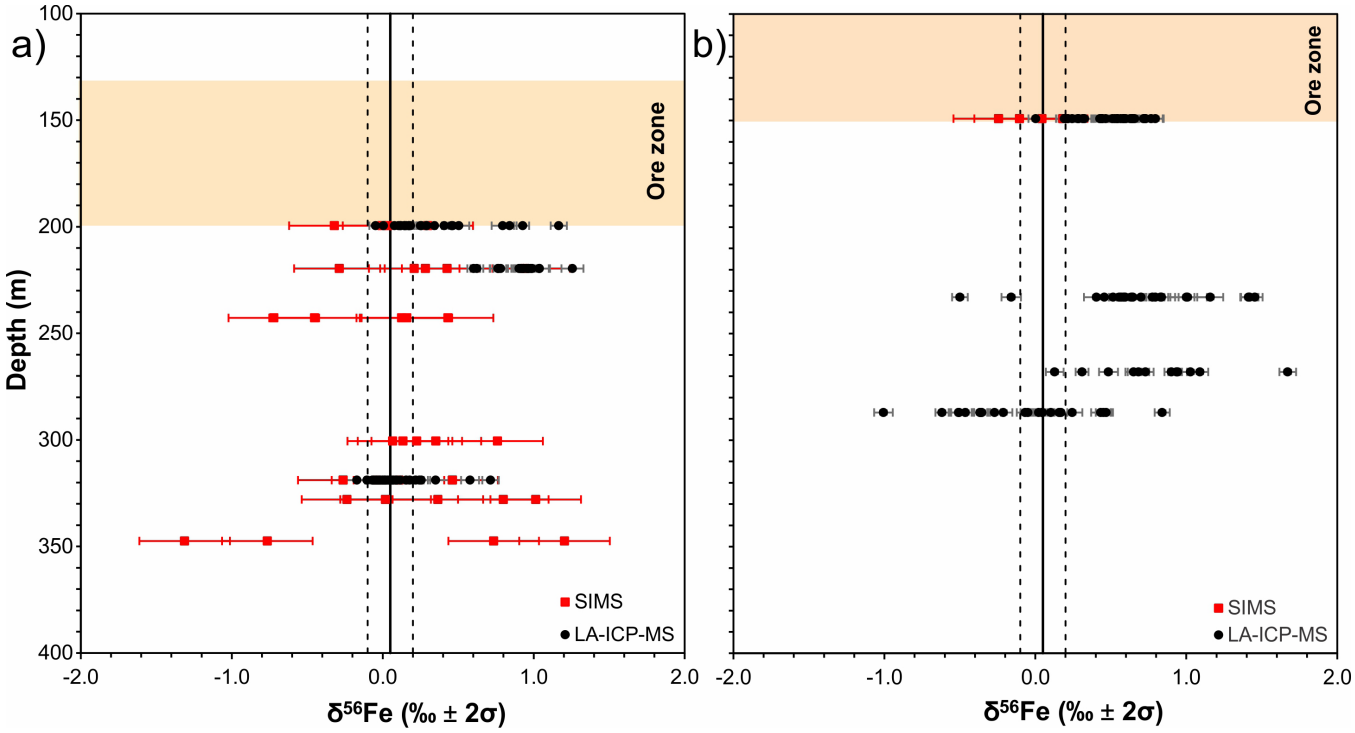

Figure 16. Iron-isotope values of samples collected from two drillholes intersecting the Triple R deposit: **a)** PLS14-175 and **b)** PLS14-177 (*after* Mount, 2019). Solid line and dashed lines represent the mean and 5th and 95th percentiles of δ^{56}Fe values, respectively, of magmatic sulfides from mafic to ultramafic rocks (Craddock and Dauphas, 2010).

$$\delta^{11}B = 1000 \times [(R_{Corr}/R_{SRM951}) - 1] \quad (4)$$

where R_{Corr} is the IMF corrected isotopic ratio and R_{SRM951} is the reference value. The strong enrichment of boron in the crust and its affinity for fluid phases, coupled with the significant difference in the δ^{11}B of distinct geological reservoirs, make boron a powerful tool for tracing hydrothermal fluids in metasomatic processes. Magmatic-dominated systems have boron isotopic compositions similar to continental magmatic arc rocks (δ^{11}B <0‰), whereas systems that derive fluids from regional evaporates, involve seawater or marine brines have highly positive δ^{11}B values (Marschall and Jiang, 2011; Tornos et al., 2012). As a result, the chemical and isotopic composition of tourmaline has proved fruitful for understanding of the source of boron and tracing fluid pathways. Tourmaline is resistant to chemical diffusion (van Hinsberg and

Marschall, 2007) and isotope homogenization, even at high pressures and temperatures. This means that regardless of post-crystallization pressure-temperature conditions or fluid compositions, chemical and isotopic heterogeneities are commonly preserved until upper amphibolite-facies conditions (van Hinsberg et al., 2011).

The boron isotope composition of tourmaline was measured using a SHRIMP II at the Geological Survey of Canada (Ottawa, Ontario), following methods outlined in Adlakha et al. (2017) and Kelly et al. (2020). Three distinct magnesio-foitite tourmaline populations (Tur 1–3) were observed from the Triple R deposit (Fig. 17). Tur 1 forms aggregates of fine-grained, prismatic to acicular crystals up to 15 µm wide and 5 to 500 µm long. These tourmaline grains can be colourless or pleochroic blue to brown. The $\delta^{11}B$ of Tur 1 typically ranges from 19.4 to 26.0‰ (n = 13), with one analysis of 16.3‰. The median of Tur 1 values across all Triple R samples is 23.1‰. Tur 1 has a distinct growth front, which acts as the nucleus for Tur 2. Visually, Tur 2 is similar to Tur 1 but textures indicate that it postdates Tur 1, forming aggregates of prismatic tourmaline that nucleated on Tur 1 and terminate within clay assemblages containing abundant illite, sudoite, and a very fine-grained (approximately 5 µm), prismatic tourmaline (Tur 3). Tur 2 has $\delta^{11}B$ values ranging from 16.3 to 19.9‰ (n = 22), plus a single analysis of 21.4‰. Intra-sample variation is low; analyses within each sample vary by less than 1‰ with the exception of two samples, which differ by approximately 1.5‰. By volume, Tur 3 is the most abundant and is responsible for the green colour observed in hand specimen; however, the fine-grained, intergrown nature of the Tur 3 crystals makes identifying individual crystals hard to distinguish. Given the small size of Tur 3 relative to the analytical spot size and possible crystal-edge effects, analyses were minimal and occurred on areas characterized by densely packed tourmaline; the values presented represent the average of many small grains interpreted to have formed synchronously and may include grain-boundary effects. The three analyses of Tur 3 are from a single sample and have $\delta^{11}B$ values of 16.0, 17.3, and 19.6‰.

The boron isotopic composition of tourmaline from the Triple R deposit clearly supports the petrographic observations that Tur 1 and Tur 2 record two unique tourmaline-forming events, each characterized by its own boron isotopic composition (Fig. 18a). Tur 1 and Tur 2 have median $\delta^{11}B$ values of 23.1 and 19.0‰, respectively, and Tur 3 overlaps with the composition of Tur 2. These isotopic compositions of tourmaline overlap results from the McArthur River deposit in the eastern Athabasca Basin (Fig. 18b; Adlakha et al., 2017). The data clearly demonstrate that the earliest generation of tourmaline present at the deposit is isotopically heavy, and later generations of tourmaline become increasingly enriched in lighter boron. A model for the boron isotopic systems of the Patterson Lake corridor mirrors Mercadier et al. (2012), in which NaCl-rich and/or $CaCl_2$-rich brines enriched in boron and magnesium by seawater evaporation have highly positive $\delta^{11}B$ values. These positive $\delta^{11}B$ brines interacted with, and leached boron from, surrounding basement rocks characterized by negative $\delta^{11}B$ values to achieve the intermediate $\delta^{11}B$ values of the hydrothermal tourmaline precipitated in the deposits. This process continued as the system developed, with later tourmaline becoming isotopically lighter (reflecting greater basement fluid interactions). Sources of boron in the basement include

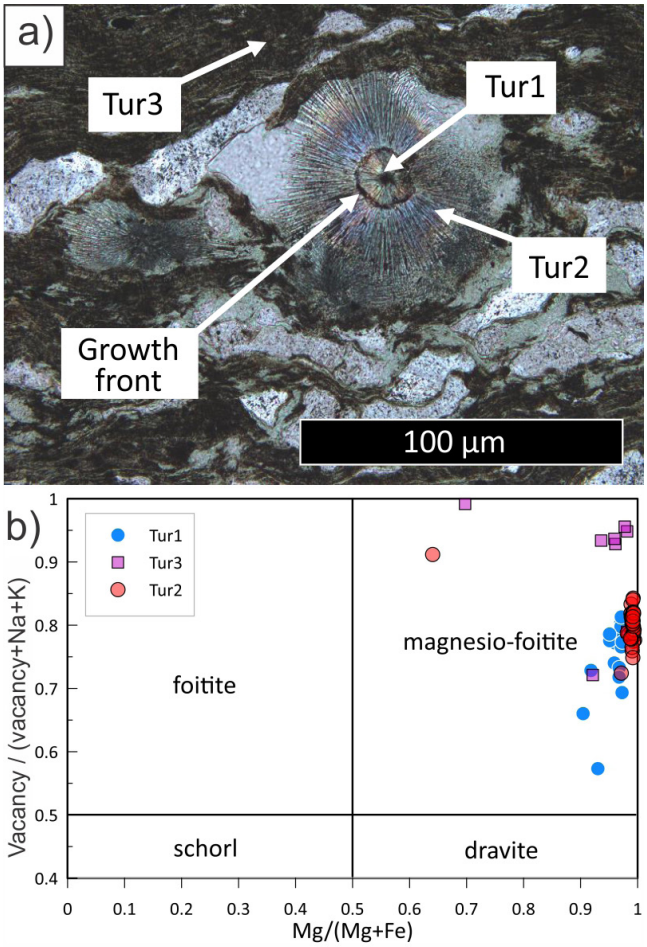

Figure 17. a) Representative photomicrograph of tourmaline morphology and distribution; **b)** classification of all generations of tourmaline from the Triple R deposit as magnesio-foitite based on the tourmaline discrimination plot of Henry et al. (2011) using Selway and Xiong (unpub. rept., 2002).

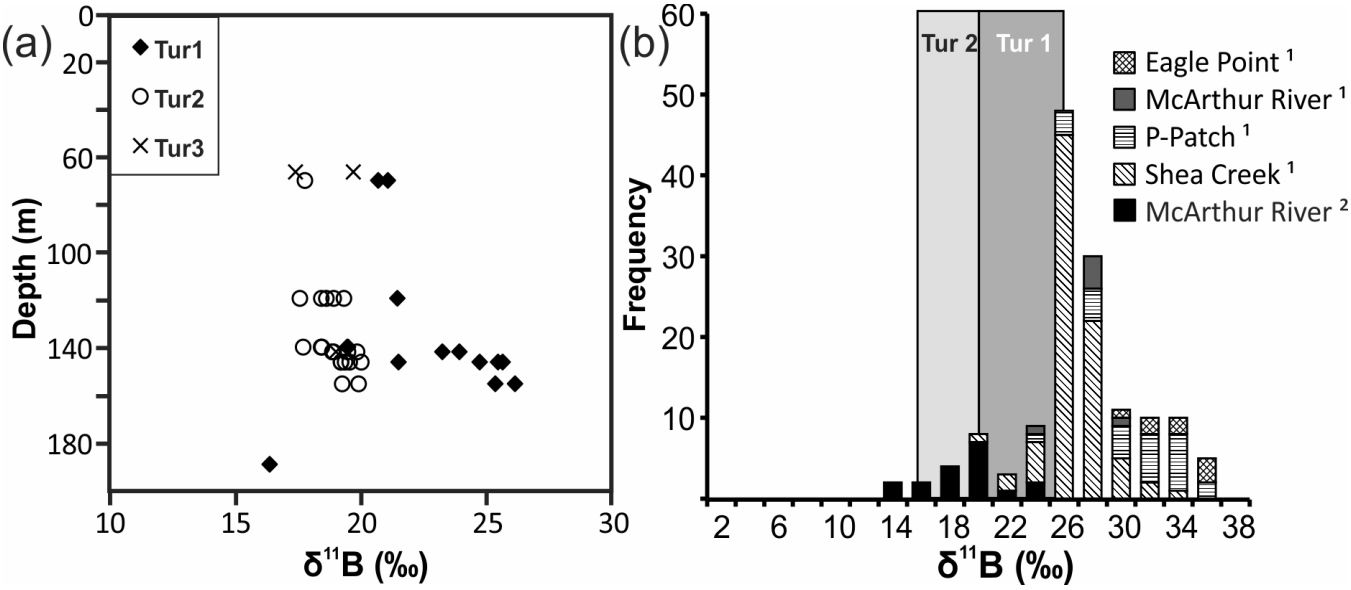

Figure 18. a) Boron isotopic composition of tourmaline populations (Tur 1, Tur 2, Tur 3) from the Triple R deposit as a function of sample depth; **b)** frequency distribution plot of tourmaline boron isotopic compositions from the Triple R deposit (this study) compared to deposits of the eastern Athabasca Basin ([1] Mercadier et al., 2012; [2] Adlakha et al., 2017).

feldspars and biotite/muscovite, which react readily with fluids and are strongly altered proximal to the Patterson Lake corridor ore zones yet contain much lower concentrations of boron than the brines. For basement-hosted deposits in the eastern Athabasca Basin, Mercadier et al. (2012) suggested that the role of basement boron was minimal, whereas Adlakha et al. (2017) proposed that initial ^{11}B enrichment due to groundwater dissolution of evaporitic and carbonate sequences was subsequently amplified by the preferential incorporation of ^{10}B into illite. Results from the Triple R deposit (this study; Kelly et al., work in progress), however, clearly demonstrate the opposite trend to Adlakha et al. (2017): the earliest generation of tourmaline at the deposit is isotopically heavy (basinal source) and later generations of tourmaline become increasingly enriched in lighter ^{10}B, reflecting great contributions from basement-derived boron. Recently, Gigon et al. (2019) proposed that the approximately 8‰ shift in $\delta^{11}B$ results between Mercadier et al. (2012) and Adlakha et al. (2017) from the McArthur River uranium deposit likely reflect matrix-dependent mass fractionation of boron isotopes during the SIMS analysis by Mercadier et al. (2012). This shift would have exaggerated any apparent basinal contribution in the models and, if applied to the eastern Athabasca data, yields $\delta^{11}B$ values similar to the Triple R deposit, reported herein.

THERMOCHRONOLOGY OF THE SOUTHWESTERN ATHABASCA BASIN

Crystalline basement rocks of the southern Rae Province have experienced a protracted geological history, including high-grade metamorphism at ca. 1.9 Ga (Card et al., 2014; Powell et al., 2018a, b), and subsequent burial underneath the Paleo- to Mesoproterozoic Athabasca Basin (e.g. Creaser and Stasiuk, 2007; Jeanneret et al., 2017), and Devonian and Cretaceous strata of the Western Canada Sedimentary Basin (Bosman et al., 2018). Published radiometric dates of uraninite and clay alteration associated with mineralization in the basin span ca. 1590 to 60 Ma (e.g. Alexandre et al., 2009), and represent the remobilization or isotopic resetting of uranium during episodic thermal-fluid activity, potentially connected with far-field tectonic events (Chi et al., 2018). This cryptic tectonothermal history is evident in the Patterson Lake corridor, where linear outliers of Devonian and Cretaceous strata (Bosman et al., 2018) indicate that the structural corridor was a topographic low, and possibly structurally reactivated, throughout the Phanerozoic. Likewise, organic thermal-maturity values (vitrinite reflectance equivalent, % R_o) measured from Cretaceous tarry bitumen that impregnate Athabasca sandstones at Hook Lake are anomalously high (<0.9% R_o) relative to background levels (0.45–0.65% R_o; Wilson et al., 2002, 2007), implying unique geothermal conditions. To better understand the thermal history of the Patterson Lake corridor,

Powell et al. (work in progress) conducted zircon (U-Th)/He dating (ZHe) on a suite of samples of crystalline basement from the southwestern Athabasca Basin margin. Two samples were collected from Taltson Domain outcrops to provide a regional cooling signature, and four samples from drill core constrain the local thermal history of the Patterson Lake corridor (Fig. 19a).

The aforementioned (U-Th)/He thermochronology is a powerful tool for quantifying the time-temperature history of geological processes. In accessory minerals such as zircon and apatite, radiogenic ^{4}He produced during the radioactive decay of ^{238}U, ^{235}U, ^{232}Th, and ^{147}Sm undergoes thermally activated diffusion through the crystal lattice at upper crustal-temperature regimes (Farley, 2000; Reiners et al., 2002). Although (U-Th)/He data are commonly reported as cooling ages, recording the time at which the mineral cooled below its corresponding closure temperature of approximately 70°C for apatite (Farley, 2000) and 185°C for zircon (Reiners et al., 2002; Wolfe and Stockli, 2010) requires a monotonic cooling history from high to low temperatures (Reiners and Brandon, 2006). Instead, rocks with protracted or multi-episodic cooling histories at temperatures below 200°C exhibit complex relationships between (U-Th)/He thermochronometer dates and grain-specific parameters that influence helium diffusion, such as grain size (Farley, 2000; Reiners et al., 2002) and radiation-damage accumulation and annealing (Flowers et al., 2009; Gautheron et al., 2009; Guenthner et al., 2013).

Previously published apatite and zircon (U-Th)/He (AHe and ZHe, respectively) thermochronology data from the Tantato Domain along the northeast margin of the Athabasca Basin span 120 ± 10 to 950 ± 50 Ma (AHe; n = 47) and 1330 ± 60 to 1730 ± 80 Ma (ZHe; n = 10), respectively (Fig. 19a; Flowers et al., 2006b; Flowers, 2009). Powell et al. (work in progress) reinterpreted these data using modern inverse numerical modelling techniques to demonstrate a protracted thermal history where rocks from the Tantato Domain were at the surface prior to deposition of the Athabasca Basin, buried to temperatures of less than 200°C during the Mesoproterozoic, and subsequently exhumed. This region was reheated to temperatures of less than 50°C in the Paleozoic and Mesozoic, attributed to burial under a ≥1 km thick section of Western Canada Sedimentary Basin strata that has since eroded (Flowers, 2009; Powell et al., work in progress). Comparatively, new ZHe data from the southwestern margin of the Athabasca Basin are dispersed from 14 ± 1 to 1954 ± 156 Ma, with most ages younger than 100 Ma (Fig. 19b). This extreme date dispersion is related to the degree of zircon-specific

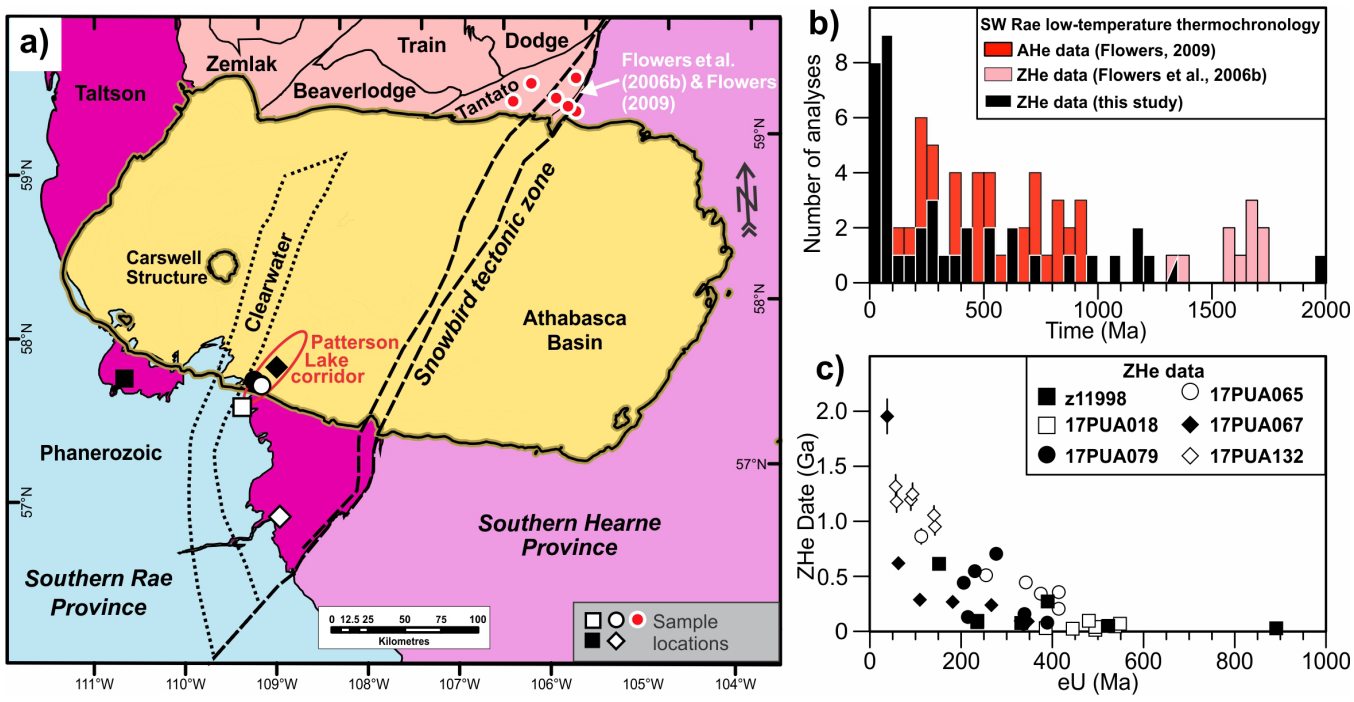

Figure 19. a) Location of thermochronology samples from the Patterson Lake corridor, Taltson Domain, and Tantato Domain; **b)** apatite and zircon (U-Th)/He (AHe and ZHe, respectively) thermochronology data, including previously published AHe and ZHe from the Tantato Domain (Flowers et al., 2006a; Flowers, 2009); and **c)** correlation of ZHe date (with two-sigma error bars) and effective uranium (eU) from the Taltson Domain (*after* Powell et al., 2019).

radiation damage, as demonstrated by the negative correlation between ZHe dates and effective uranium (eU) concentrations (Fig. 19c).

Powell et al. (work in progress) used the numerical-modelling software HeFTy (Ketcham, 2005) to investigate the time-temperature implications of these ZHe date–eU concentration trends (Fig. 19c), which indicate that some samples from the Patterson Lake corridor were subject to elevated temperatures (approximately 160°C) from the Cretaceous to Present, relative to samples from the Taltson Domain and northeast of the Athabasca Basin. It is unlikely that these temperatures reflect burial heating under a standard geothermal gradient because that would require a greater than 5 km thick package of Cretaceous to Paleogene sediments, which is counter to the depositional trends and other estimates of an eroded thickness of 1 to 3 km of pre-Eocene sediments from the Western Canada Sedimentary Basin (Dawson et al., 1990; Stasiuk et al., 2006; Flowers, 2009). Instead, Powell et al. (work in progress) invoke elevated geothermal conditions potentially related to buried, high-heat–producing granitic suites such as the Clearwater Domain (Fig. 6). Anomalous geothermal gradients in excess of 50°C/km are documented in Western Canada Sedimentary Basin strata adjacent to the Athabasca Basin, and are attributed to high RHP from the basement (Bachu and Burwash, 1994). A similarly steep geothermal gradient may have developed proximal to the Clearwater Domain throughout the Phanerozoic, when sedimentary strata of the Western Canada Sedimentary Basin blanketed the basement rocks of the southwestern Rae Province. Additionally, elevated temperatures from the Cretaceous to Present could reflect circulation of hot hydrothermal fluids from depth along the vertical fault systems in the structural corridor. The variability of ZHe dates and model results from proximal drill cores (e.g. 17PUA065 and 17PUA079 from the Spitfire discovery) may reflect local-scale convective heat transfer, where rocks adjacent to major fluid conduits are subject to higher temperature regimes.

DISCUSSION

Similar to the eastern Athabasca Basin uranium deposits (e.g. Alexandre et al., 2009), preliminary uraninite U-Pb geochronology from the Arrow deposit indicates primary mineralization occurred at ca. 1.4 Ga, with numerous younger isotopic disturbances (Hillacre et al., 2019). These results align with numerical AHe and ZHe thermodynamic modelling that records a protracted thermal history in the Patterson Lake corridor. During these periods, hydrothermal fluids were focused to great depths in the basement during brittle-ductile and brittle deformation events, with total homogenization temperatures of fluid inclusions preserved in drusy quartz veins reaching 250°C (Fig. 13a). Of particular importance are late west- and north-northwest–striking brittle conjugate faults that crosscut the Athabasca sandstone and provided pathways for uranium-bearing fluids to precipitate metals along reactivated northeast-striking brittle-ductile structures (Johnstone et al., 2019, work in progress). As illustrated by the extreme variation in iron isotope values associated with uranium mineralization, these fluid migrations induced multiple generations of pyrite dissolution-reprecipitation and redox reactions. Fault-valve behaviour (Sibson, 1990) is one mechanism to explain the localized, alternating reduced and oxidized conditions wherein the faults become highly permeable immediately post-failure (oxidized) but seal during the interseismic period (reduced). As proposed by Chi et al. (2018), however, the low concentrations of non-aqueous volatiles in the vapour phase and low fluid pressures associated with boiling (Chi et al., 2014, 2017; Liang et al., 2017; Wang et al., 2018) are better explained by the suction pump model that is typical of epithermal-style systems (Sibson, 1987; Sibson et al., 1988), in which a fluid-pressure regime fluctuates between hydrostatic and subhydrostatic, rather than between lithostatic and hydrostatic, during fault-valve–controlled fluid flow (Sibson, 1987; Sibson et al., 1988). Under normal geothermal gradients, a fluid with 25 weight per cent NaCl cannot boil at the temperatures indicated by the fluid inclusion data. The only mechanism to explain the boiling is by faulting, which causes rapid changes in pressure (Chi et al., 2014, 2017; Wang et al., 2018; Rabiei et al., 2019; Rabiei et al., work in progress).

In the Patterson Lake corridor, the evolution of salinity and X_{NaCl} through time recorded in the various generations of quartz veining suggests that hydrothermal fluids with high salinities and high levels of $CaCl_2$ developed during deposition of the Athabasca Supergroup and uranium mineralization, consistent with a basinal origin for the brines (Chu and Chi, 2016). Although alteration of the basement could account for the higher salinities and $CaCl_2$-rich fluids, a natural outcome of the classic Hoeve and Sibbald (1978) model, development of $CalCl_2$-rich brines within the basin and at different depths in the basement in the Patterson Lake corridor area is consistent with the recent finding that calcium-rich uraniniferous diagenetic fluids were developed within the Athabasca Basin (Chi et al., 2019). The boron isotopic composition of tourmaline and isotopic changes with respect to distinct tourmaline generations also support the incursion of basinal brines, enriched in boron and magnesium by seawater evaporation, that

interacted with the surrounding basement rocks. This process caused later generations of tourmaline to become isotopically lighter as the systems evolved.

Regional geophysical modelling has identified several new features including crustal-scale structures and undated felsic intrusions. One of the structures is situated at a critical junction between the Clearwater, Tantato, and Taltson domains and may have played a role in localizing heat and fluid flow in the Patterson Lake corridor. Given the extent of radiogenic heat-producing 1.84 Ga Clearwater Domain granites (Fig. 4, 5), the newly recognized structures and felsic intrusions may have contributed to sustained and elevated geothermal gradients as indicated by the zircon (U-Th)/He thermochronology data and could have played a role in remobilizing elements associated with a conductivity anomaly below the Clearwater Domain and uranium deposits (Fig. 4). Similar lithospheric conductivity highs present in the northeastern Rae Province have been attributed to mantle melt and metasomatic components associated with intrusion of the Hudson granites (Spratt et al., 2014).

Weyer et al. (1989) originally proposed involvement of magmatic fluids from Hudson granite intrusions in the formation of the Lone Gull (Kiggavik) uranium deposits in Thelon Basin based on spatial associations between the granite intrusions, mineralization, and oxygen isotope compositions of illite and uraninite; however, U-Pb geochronology of uraninite revealed much younger ages, from 1403 ± 10 Ma (A. Farkas, unpub. rept., 1984) to 489 ± 16 Ma (Shabaga et al., 2017) compared to the 1850 to 1810 Ma Hudson suite (Peterson and van Breemen, 1999), whereas K-Ar and $^{40}Ar/^{39}Ar$ dates from hydrothermal illite range from 1330 ± 36 Ma (Shabaga et al., 2017) to 913 ± 7 Ma (Weyer, 1992). Although the age constraints rule out direct involvement of Paleoproterozoic magmatic fluids and heat in the ores, the Hudson and Nueltin suites, located in the Rae Province, have significant RHP (Fig. 6; median values of 11.67 and 6.71 μWm^{-3}, respectively, calculated from data in Peterson et al. [2002], Scott [2012], and Scott et al. [2015]). Samples of Hudson granites recently documented from the southern Rae Province of the Northwest Territories, north of the Athabasca Basin, also have anomalously high RHP (Fig. 6; median value of 4.81 μWm^{-3}, calculated from data in Peterson et al. [in press]).

Fehn et al. (1978) developed the first numerical models indicating that RHP from fractured granites could induce hydrothermal convection and generate large uranium deposits. The applicability of these models are generally supported by the presence of modern hotsprings along major fault systems in the 100 to 60 Ma Idaho batholith (Fyfe, 1973; Bennett, 1980; Hyndman, 1981; Bennett and Knowles, 1985) and surrounding Paleogene granites (Young, 1985). At the Idaho batholith, several studies have proposed that radiogenic decay in tonalitic to granitic Cretaceous phases and dioritic Paleogene granitoids is the thermal source for 50 to 225°C hotspring waters (Kuhns, 1980; Young, 1985; Vance, 1986; van Middlesworth and Wood, 1998) and nearby hydrothermal vein deposits (e.g. the Snowbird REE±Th±fluorite deposit [Metz et al., 1985; Samson et al., 2004], Lemhi Pass Th±REE deposit [Anderson, 1961; Staatz, 1972], and several uranium occurrences [Anderson, 1958; Della Valle, 1975]). In these environments, the maximum depth of fluid circulation has been estimated to be 2.4 to 6.7 km, yielding a geothermal gradient of approximately 50°C/km (Kuhns, 1980; Druschel and Rosenberg, 2001). Brittle fault zones with elevated metal contents in the Clearwater granite intrusions (Fig. 7) clearly align with geothermal-induced fluid flow. Bearing these models in mind, heat production would have been originally higher than present-day values due to radiogenic decay, while the regional geothermal gradient was likely enhanced by burial and overlap by several kilometres of basin fill (i.e. Athabasca and Thelon basins). For example, high-heat–producing granites buried beneath insulating sedimentary sequences in the Mount Isa inlier in Australia have been shown to generate steep upper-crustal thermal gradients (McLaren et al., 1999).

CONCLUSIONS – AN INTEGRATED GENETIC MODEL

A genetic model that encompasses these elements in presented in Figure 20. The model builds on the classic Hoeve and Sibbald (1978) and Kyser and Cuney (2009) models to include the Clearwater Domain and other felsic intrusions as heat sources for the basin brines, rather than heating of the basin brines through burial to depths of approximately 5 to 6 km as proposed by Pagel (1975) and Hoeve and Sibbald (1978). Chi et al. (2018) note that geochronostratigraphic constraints indicate that the unconformity surface was likely at less than 3 km of depth during the primary ca. 1.5 Ga mineralization event. The thermochronology results indicate a sustained, elevated geothermal gradient that had the potential to drive fluid flow when the region was covered by extensive sedimentary units in the Mesoproterozoic and Cretaceous to the Paleogene. Although incursion of petroleum-bearing brines during deposition of the Western Canada Sedimentary Basin

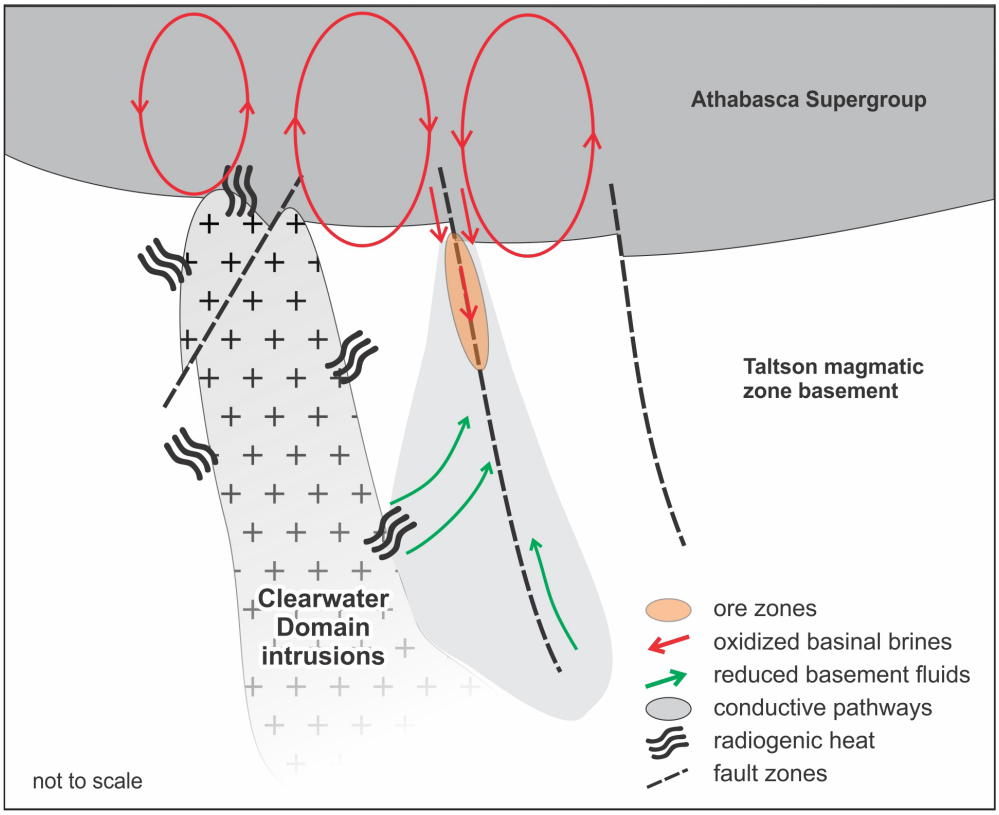

Figure 20. Conceptual genetic model for the Patterson Lake corridor uranium deposits. The high-heat–producing Clearwater Domain and other felsic intrusions formed hydrothermal cells centred over the fault zones (e.g. Li et al., 2016) that led to oxidized brines interacting with sulfide-bearing ultramafic to mafic rocks in the basement along the reactivated fault zone. Uranium precipitation was induced by pressure changes that caused boiling during fault reactivations and reduction-oxidation reactions between the uranium-bearing oxidized brines, sulfide-bearing host rocks, and possibly basement-derived fluids.

may not have contributed to the uranium endowment, they may have prevented dissolution and remobilization of the high-grade ores by oxidized fluids and explain the presence of pyrobitumen in the deposits (Hoeve and Sibbald, 1978; Wilson et al., 2007). This is consistent with results throughout the Athabasca Basin, where despite uraninite U-Pb geochronology producing a wide range of ages from 1590 to 61 Ma (e.g. Alexandre et al., 2009), the events causing these younger isotopic resetting were unlikely to add significant uranium to the deposits (Martz et al., 2017) and only caused localized remobilization. Other theories for the presence of pyrobitumen in the ores include catalytic hydrogenation of CO_2 (Sangély et al., 2007), radiolysis of basement graphite (Kyser et al., 1989), and dehydrogenation and polymerization of graphite (Landais et al., 1993); however, as Wilson et al. (2007) note, pyrobitumen includes and crosscuts the uranium ores, indicating that its formation postdates ore-forming processes.

Previous studies have proposed uranium-enriched granites and granitic pegmatites in the underlying basement were potential metal sources for the deposits (e.g. Thomas, 1983; Annesley et al., 1997; Annesley and Madore, 1999; Hecht and Cuney, 2000; Cuney, 2005; Richard et al., 2010), with brine percolation into the basement enhanced by faults and microfracture networks (Mercadier et al., 2010, 2013; Martz et al., 2018). Although these studies have emphasized the role of the basement rocks as uranium sources, intrusive Clearwater suites and other undated felsic intrusions below the Athabasca and Thelon basins have also provided radiogenic heat to generate a sustained, elevated geothermal gradient throughout the basins and localized thermal anomalies above conductive fault zones (e.g. Li et al., 2016). In addition to the Clearwater Domain granites, heat-producing sources underlying the basin include 1840 to 1810 Ma Trans-Hudson Orogen biotite-bearing monzogranite to tonalite plutons and granitic pegmatites (Annesley et al., 2005; McKechnie et al., 2013), and ca. 1820 to 1800 Ma and ca. 1.8 Ga granitic plutons along the Virgin River shear zone (Bickford et al., 1990, 1994; Card et al., 2002). An elevated geothermal gradient permits shallower depths of mineralization as proposed by Chi et al. (2018) and is supported by the presence of open-space textures (e.g. breccias, dissolution vugs, and drusy veins reported by Hoeve and Quirt [1984], Jefferson et al. [2007], and Kyser and Cuney [2015]) and evidence of fluid boiling in the deposits (this study; Chi et al., 2014, 2018; Liang et al., 2017; Wang et al., 2018; Rabiei et al., 2019, work in progress). These extensive heat and uranium sources, coupled with basin-wide uranium-bearing brines as documented by Chi et al. (2019), support the hypothesis that efficient reducing media in reactivated fault zones in the basement rocks are critical to localizing the deposits. In the Patterson

Lake corridor, isotopic, textural, and fluid inclusion data indicate that boiling induced by drastic fluid-pressure changes and redox reactions between sulfide minerals, ferromagnesian minerals, and fluids caused the ores to precipitate along reactivated shear zones. As revealed by the MT survey, these shear zones have deep, conductive roots that extend to the mantle and require further study.

HIGHLIGHTS OF THE TGI URANIUM FLUID PATHWAYS ACTIVITY

- New geophysical surveys over prospective corridors in Saskatchewan and Alberta define geological domains beneath the western Athabasca Basin, including recognizing new crustal-scale structures, intrusions, and expanding the extent of the Clearwater Domain.
- Fluid inclusion studies highlight similarities between the Patterson Lake corridor deposits and the eastern Athabasca Basin deposits, e.g. the presence of NaCl- and $CaCl_2$-rich fluids; evidence of fluid boiling.
- New structural interpretations highlight the complex history of the corridor and role of late west- and north-northwest–striking brittle conjugate faults in providing pathways for uranium-bearing fluids to precipitate metals along reactivated northeast-striking brittle-ductile structures.
- Isotopic data from pyrite record significant fluid-rock interactions and element recycling during fluctuating oxidized and reduced conditions along the fault-controlled ore zones.
- Boron isotopic studies of tourmaline from the Arrow deposit support incursion of marine basinal brines to great depths in the basement and interaction of those brines with the basement rocks.
- Zircon (U-Th)/He thermochronology modelling records elevated temperatures (approximately 160°C) during the deposition of Cretaceous to Paleogene sediments, which is counter to depositional trends and other estimates of eroded thickness, supporting the need for a sustained heat source.
- The association of high-radiogenic-heat–producing Clearwater Domain granitic intrusions and other ca. 1.8 Ga felsic intrusions with known uranium mineralization and anomalies.
- A revised genetic model for the Patterson Lake corridor uranium-related deposits wherein high-heat–producing intrusions warmed hydrothermal fluids that were focused along pre-existing ductile deformation corridors. Fault-valve action during brittle deformation induced flash-boiling, fluid-rock interactions, and ultimately metal precipitation.
- Confirmation that mineralization can extend up to 1 km below the unconformity surface — significantly expanding the mineral potential of the regions surrounding and linking the Proterozoic basins.

ACKNOWLEDGMENTS

This paper summarizes key results of the Uranium Fluid Pathways activity of the TGI program, delivered by the Geological Survey of Canada in collaboration with the Saskatchewan and Alberta geological surveys. Purepoint Uranium Group Ltd. and their Joint Venture partners Orano Canada and Cameco Corp., Forum Energy Metals Corp., NexGen Energy Limited, Fission Uranium, and CanAlaska Uranium generously provided logistical support and shared geological data and knowledge. Big Bear Contracting and Canadian Helicopters provided additional logistical support. C. Duffett and S. Mount assisted with field data collection. Constructive peer reviews by Gerard Zaluski and Tony Peterson greatly improved this report. Scientific editing and layout services were provided by Purple Rock Inc.

REFERENCES

Acevedo, A. and Kyser, T.K., 2015. Fe isotopic composition of alteration minerals from McArthur River Zone 4 deposit, Athabasca Basin, Saskatchewan; *in* Targeted Geoscience Initiative 4: unconformity-related uranium systems, (ed.) E.G. Potter and D.M. Wright; Geological Survey of Canada, Open File 7791, p. 61–73. https://doi.org/10.4095/295776

Adlakha, E.E., Hattori, K., Davis, W.J., and Boucher, B., 2017. Characterizing fluids associated with the McArthur River U deposit, Canada, based on tourmaline trace element and stable (B, H) isotope compositions; Chemical Geology, v. 466, p. 417–435. https://doi.org/10.1016/j.chemgeo.2017.06.030

Alexandre, P., Kyser, T.K., Polito, P., and Thomas, D., 2005. Alteration mineralogy and stable isotope geochemistry of Paleoproterozoic basement-hosted unconformity-type uranium deposits in the Athabasca Basin, Canada; Economic Geology, v. 100, no. 8, p. 1547–1563. https://doi.org/10.2113/gsecongeo.100.8.1547

Alexandre, P., Kyser, K., Thomas, D., Polito, P., and Marlat, J., 2009. Geochronology of unconformity-related uranium deposit in the Athabasca Basin, Saskatchewan, Canada, and their integration in the evolution of the basin; Mineralium Deposita, v. 44, p. 41−59. https://doi.org/10.1007/s00126-007-0153-3

Alexandre, P., Kyser, K., Jiricka, D., and Witt, G., 2012. Formation and evolution of the Centennial unconformity-related uranium deposit in the south-central Athabasca Basin, Canada; Economic Geology, v. 107, no. 3, p. 385–400. https://doi.org/10.2113/econgeo.107.3.385

Alwmark, C., Bleeker, W., Lecheminant, A., Page, L., and Scherstén, A., 2017. An Early Ordovician ^{40}Ar-^{39}Ar age for the ~50 km Carswell impact structure, Canada; Geological Society of America Bulletin, v. 129, no. 11–12, p. 1442–1449. https://doi.org/10.1130/B31666.1

Anderson, A.L., 1958. Uranium, thorium, columbium and rare earth deposits in the Salmon region, Lemhi County, Idaho; Idaho Bureau of Mines, Geology Pamphlet P-115, 94 p.

Anderson, A.L., 1961. Thorium mineralization in the Lemhi Pass area, Lemhi County, Idaho; Economic Geology, v. 56, no. 1, p. 177–197. https://doi.org/10.2113/gsecongeo.56.1.177

Annesley, I.R. and Madore, C., 1999. Leucogranites and pegmatites of the sub-Athabasca basement, Saskatchewan: U protore? *in* Mineral deposits, processes to processing: proceedings of the fifth biennial SGA meeting and the tenth quadrennial IAGOD symposium, London, United Kingdom, 22–25 August 1999, (ed.) C.J. Stanley; Balkema, Rotterdam, Netherlands, p. 297–300 (extended abstract).

Annesley, I.R., Madore, C., Shi, R., and Krogh, T.E., 1997. U-Pb geochronology and thermotectonic events in the Wollaston Lake area, Wollaston Domain: a summary 1994–1996; *in* Summary of Investigations 1997; Saskatchewan Ministry of Energy and Mines, Saskatchewan Geological Survey, Miscellaneous Report 97-4, p. 162–173.

Annesley, I.R., Madore, C., and Portella, P., 2005. Geology and thermotectonic evolution of the western margin of the Trans-Hudson Orogen: evidence from the eastern sub-Athabasca basement, Saskatchewan; Canadian Journal of Earth Sciences, v. 42, no. 4, p. 573–597. https://doi.org/10.1139/E05-034

Ashton, K.E., Hartlaub, R.P., Bethune, K.M., Heaman, L.M., Rayner, N. and Niebergall, G.R., 2013. New depositional age constraints for the Murmac Bay group of the southern Rae craton, Canada; Precambrian Research, v. 232, p. 70–88. https://doi.org/10.1016/j.precamres.2012.05.008

Ashton, K.E., Rayner, N.M., Heaman, L.M., and Creaser, R.A., 2014. New Sm-Nd and U-Pb ages from the Zemlak and south-central Beaverlodge domains: a case for amalgamated Taltson basement complex and proto-Rae cratonic blocks within the Rae Province of Northwestern Saskatchewan; *in* Summary of Investigations 2014, volume 2; Saskatchewan Ministry of the Economy, Saskatchewan Geological Survey, Miscellaneous Report 2014-4.2, Paper A-6, 28 p.

Ashton, K., Knox, B., Rayner, N., Creaser, R., and Bethune, K., 2017. New U-Pb and Sm-Nd results from the Tantato Domain, southeastern Rae Province, Saskatchewan; *in* Summary of Investigations 2017, volume 2; Saskatchewan Ministry of the Economy, Saskatchewan Geological Survey, Miscellaneous Report 2017-4.2, Paper A-14, 27 p. and 3 Excel files.

Ashton, K., Card, C., and Rayner, N., 2018. A new U-Pb age for the Hudson granites and lamprophyre dykes in the southern Rae Province of Saskatchewan; *in* Summary of Investigations 2018, volume 2; Saskatchewan Ministry of Energy and Resources, Saskatchewan Geological Survey, Miscellaneous Report 2018-4.2, Paper A-6, 15 p.

Bachu, S. and Burwash, R.A., 1994. Geothermal regime in the Western Canada Sedimentary Basin; Chapter 30 *in* Geological atlas of the Western Canada Sedimentary Basin, (comp.) G.D. Mossop and I. Shetsen; Canadian Society of Petroleum Geologists and Alberta Research Council, p. 447–454.

Bast, R., Scherer, E.E., Mezger, K., Austrheim, H., Ludwig, T., Marschall, H.R., Putnis, A., and Löwen, K., 2014. Boron isotopes in tourmaline as a tracer of metasomatic processes in the Bamble sector of Southern Norway; Contributions to Mineralogy and Petrology, v. 168, 1069. https://doi.org/10.1007/s00410-014-1069-4

Beard, B.L. and Johnson, C.M., 2004. Fe isotope variations in the modern and ancient Earth and other planetary bodies; Reviews in Mineralogy and Geochemistry, v. 55, p. 319–357. https://doi.org/10.2138/gsrmg.55.1.319

Bennett, E.H., 1980. Granitic rocks of Tertiary age in the Idaho batholith and their relation to mineralization; Economic Geology, v. 75, no. 2, p. 278–288. https://doi.org/10.2113/gsecongeo.75.2.278

Bennett, E.H. and Knowles, C.R., 1985. Tertiary plutons and related rocks in central Idaho; *in* Symposium on the geology and mineral deposits of the Challis 1 degree × 2 degrees quadrangle, Idaho, (ed.) D.H. McIntyre; U.S. Geological Survey, Bulletin 1658 A-S, p. 81–95. https://doi.org/10.3133/b1658AS

Bethune, K.M., Hunter, R.C., and Ashton, K.E., 2010. Age and provenance of the Paleoproterozoic Thluicho Lake Group based on detrital zircon U–Pb SHRIMP geochronology: new insights into the protracted tectonic evolution of the southwestern Rae Province, Canadian Shield; Precambrian Research, v. 182, no. 1–2, p. 83–100. https://doi.org/10.1016/j.precamres.2010.07.003

Bethune, K.M., Berman, R.G., Rayner, N., and Ashton, K.E., 2013. Structural, petrological and U–Pb SHRIMP geochronological study of the western Beaverlodge domain: implications for crustal architecture, multi-stage orogenesis and the extent of the Taltson Orogen in the SW Rae Craton, Canadian Shield; Precambrian Research, v. 232, p. 89–118. https://doi.org/10.1016/j.precamres.2013.01.001

Bickford, M.E., Collerson, K.D., Lewry, J.F., van Schmus, W.R., and Chiarenzelli, J.R., 1990. Proterozoic collisional tectonism in the Trans-Hudson Orogen, Saskatchewan; Geology, v. 18, no. 1, p. 14–18. https://doi.org/10.1130/0091-7613(1990)018%3C0014:PCTITT%3E2.3.CO;2t

Bickford, M.E., Collerson, K.D., and Lewry, J.F., 1994. Crustal history of the Rae and Hearne provinces, southwestern Canadian Shield, Saskatchewan: constraints from geochronologic and isotopic data; Precambrian Research, v. 68, no. 1–2, p. 1–21. https://doi.org/10.1016/0301-9268(94)90062-0

Bosman, S.A. and Ramaekers, P., 2015. Athabasca Group + Martin Group = Athabasca Supergroup? Athabasca Basin multiparameter drill log compilation and interpretation, with updated geological map; *in* Summary of Investigations 2015, volume 2; Saskatchewan Ministry of the Economy, Saskatchewan Geological Survey, Miscellaneous Report 2015-4.2, Paper A-5, 13 p.

Bosman, S.A., Noll, J., Johnson, D., and Strocen, B., 2017. Uranium geoscience in the Athabasca Basin and Western Canada Sedimentary Basin in northwestern Saskatchewan (NTS 74F and 74K); *in* Summary of Investigations 2017, volume 2; Saskatchewan Ministry of Economy, Saskatchewan Geological Survey, Miscallenous Report, 2017-4.2, Paper A-4, 14 p.

Bosman, S.A., Blampied, T.R., and Tremblay, M.P., 2018. Mapping sedimentary rocks of the Athabasca Supergroup, Elk Point Group, Mannville Group and younger diamictite in the Patterson Lake region (NTS 74F), northwest Saskatchewan; *in* Summary of Investigations 2018, volume 2; Saskatchewan Ministry of Energy and Resources, Saskatchewan Geological Survey, Miscellaneous Report 2018-4.2, Paper A-3, 29 p.

Bostock, H.H. and van Breemen, O., 1994. Ages of detrital and metamorphic zircons and monazites from a pre-Taltson magmatic zone basin at the western margin of Rae Province; Canadian Journal of Earth Sciences, v. 31, no. 8, p. 1353–1364. https://doi.org/10.1139/e94-118

Bostock, H.H., van Breemen, O., and Loveridge, W.D., 1991. Further geochronology of plutonic rocks in northern Taltson magmatic zone, District of Mackenzie, N.W.T.; *in* Radiogenic age and isotopic studies: report 4; Geological Survey of Canada, Paper 90-2, p. 67–78. https://doi.org/10.4095/131938

Bouzidi, Y., Schmitt, D.R., and Burwash, R.A., 2002. Variations in crustal thickness in Alberta from depth-migrated seismic reflection profiles; Canadian Journal of Earth Sciences, v. 39, no. 3, p. 331–350. https://doi.org/10.1139/e01-080

Bray, C., Spooner, E., Golightly, J., and Saracoglu, R., 1982. Carbon and sulphur isotope geochemistry of unconformity-related uranium mineralization, McClean Lake deposits, N. Saskatchewan, Canada; Geological Society of America, Abstracts with program, v. 14, p. 451.

Caldwell, T.G., Bibby, H.M., and Brown, C., 2004. The magnetotelluric phase tensor; Geophysical Journal International, v. 158, no. 2, p. 457–469. https://doi.org/10.1111/j.1365-246X.2004.02281.x

Card, C.D., 2002. New investigations of basement to the western Athabasca Basin; *in* Summary of Investigations 2002; Saskatchewan Industry and Resources, Saskatchewan Geological Survey, Miscellaneous Report 2002-4.2, Paper D-12, 17 p.

Card, C.D., 2016. A coming together: the juxtaposition of the Rae and Hearne cratons along the Virgin River shear zone (Snowbird tectonic zone), Saskatchewan, Canada, and the implications for proto-Laurentia; Ph.D. thesis, University of Regina, Regina, Saskatchewan, 224 p.

Card, C.D., 2017. Distribution and significance of crystalline rocks in the Patterson Lake uranium exploration corridor of northwest Saskatchewan; *in* Summary of Investigations 2017, volume 2; Saskatchewan Minstry of Energy and Economy, Saskatchewan Geological Survey, Miscellaneous Report 2017-4.2, Paper A-11, 18 p.

Card, C.D., 2018. The Patterson Lake alkaline igneous complex: evidence for deep-seated structural control in the Patterson Lake corridor and implications for mineral exploration; *in* Summary of Investigations 2018, volume 2; Saskatchewan Ministry of Energy and Economy, Sakatchewan Geological Survey, Miscellaneous Report 2018-4.2, Paper A-9, 19 p.

Card, C.D. and Noll, J., 2016. Host-rock protoliths, pre-ore metasomatic mineral assemblages and textures, and exotic rocks in the western Athabasca Basin: ore-system controls and implications for the unconformity-related uranium model; *in* Summary of Investigations 2016; Saskatchewan Ministry of the Economy, Saskatchewan Geological Survey, Miscellaneous Report 2016-4.2, Paper A-8, 19 p.

Card, C.D., Pană, D., Portella, P., Thomas, D.J., and Annesley, I.R., 2007a. Basement rocks to the Athabasca Basin, Saskatchewan and Alberta; *in* EXTECH IV: Geology and uranium EXploration TECHnology of the Proterozoic Athabasca Basin, Saskatchewan and Alberta, (ed.) C.W. Jefferson and G. Delaney; Geological Survey of Canada, Bulletin 588, p. 69–87. https://doi.org/10.4095/223745

Card, C.D., Pană, D., Portella, P., Thomas, D.J., and Annesley, I.R., 2007b. New insights into the geological history of the basement rocks to the southwestern Athabasca Basin, Saskatchewan and Alberta; *in* EXTECH IV: Geology and uranium EXploration TECHnology of the Proterozoic Athabasca Basin, Saskatchewan and Alberta, (ed.) C.W. Jefferson and G. Delaney; Geological Survey of Canada, Bulletin 588, p. 119–133. https://doi.org/10.4095/223747

Card, C.D., Bethune, K.M., Davis, W.J., Rayner, N., and Ashton, K.E., 2014. The case for a distinct Taltson Orogeny: evidence from northwest Saskatchewan, Canada; Precambrian Research, v. 255, no. 1, p. 245–265. https://doi.org/10.1016/j.precamres.2014.09.022

Cerin, D., Gotze, J., and Pan, Y., 2017. Radiation-induced damage in quartz at the Arrow uranium deposit, southwestern Athabasca Basin, Saskatchewan; The Canadian Mineralogist, v. 55, no. 3, p. 457–472. https://doi.org/10.3749/canmin.1700003

Chi, G., Liang, R., Ashton, K., Haid, T., Quirt, D., and Fayek, M., 2014. Evidence of fluid immiscibility from uranium deposits in northern Saskatchewan and Nunavut and potential relationship with uranium precipitation; Geological Association of Canada–Mineralogical Association of Canada (GAC-MAC) Annual Conference, Volume of abstracts, v. 37, p. 57.

Chi, G., Haid, T., Quirt, D., Fayek, M., Blamey, N., and Chu, H., 2017. Petrography, fluid inclusion analysis and geochronology of the End uranium deposit, Kiggavik, Nunavut, Canada; Mineralium Deposita, v. 52, no. 2, p. 211–232. https://doi.org/10.1007/s00126-016-0657-9

Chi, G., Li, Z., Chu, H., Bethune, K.M., Quirt, D.H., Ledru, P., Normand, C., Card, C., Bosman, S., Davis, W.J., and Potter, E.G., 2018. A shallow-burial mineralization model for the unconformity-related uranium deposits in the Athabasca Basin; Economic Geology, v. 113, no. 5, p. 1209–1217. https://doi.org/10.5382/econgeo.2018.4588

Chi, G., Chu, H., Petts, D., Potter, E.G., Jackson, S., and Williams-Jones, A., 2019. Uranium-rich diagenetic fluids provide the key to unconformity-related uranium mineralization in the Athabasca Basin; Scientific Reports, v. 9, 5530. https://doi.org/10.1038/s41598-019-42032-0

Chu, H. and Chi, G., 2016. Thermal profiles inferred from fluid inclusion and illite geothermometry from sandstones of the Athabasca Basin: implications for fluid flow and unconformity-related uranium mineralization; Ore Geology Reviews, v. 75, p. 284–303. https://doi.org/10.1016/j.oregeorev.2015.12.013

Cox, J.J., Robson, D.M., Mathisen, M.B., Ross, D.A., Coetzee, V., and Wittrup, M., 2017. Technical report on the preliminary economic assessment of the Arrow deposit, Rook 1 property, province of Saskatchewan, Canada; NI 43-101 technical report prepared by Roscoe Postle Associates for NexGen Energy Ltd., effective date 31 July, 2017.

Craddock, P.R. and Dauphas, N., 2010. Iron isotopic compositions of geological reference materials and chondrites; Geostandards and Geoanalytical Research, v. 35, no. 1, p. 101–123. https://doi.org/10.1111/j.1751-908X.2010.00085.x

Creaser, R.A. and Stasiuk, L.D., 2007. Depositional age of the Douglas Formation, northern Saskatchewan, determined by RE-Os geochronology; *in* EXTECH IV: Geology and uranium EXploration TECHnology of the Proterozoic Athabasca Basin, Saskatchewan and Alberta, (ed.) C.W. Jefferson and G. Delaney; Geological Survey of Canada, Bulletin 588, p. 341–346. https://doi.org/10.4095/223779

Cuney, M., 2005. World-class unconformity-related uranium deposits: key factors for their genesis; *in* Mineral deposit research: meeting the global challenge, (ed.) J. Mao and F.P. Bierlein; Springer, Berlin, Germany, p. 245–248. https://doi.org/10.1007/3-540-27946-6_64

Dawson, F.M., Evans, C., Marsh, R., and Power, B., 1990. Uppermost Cretaceous-Tertiary strata of the Western Canada Sedimentary Basin; *in* Canadian Society of Petroleum Geologists Annual Convention, Program with abstracts; Bulletin of Canadian Petroleum Geology, v. 38, no. 1, p. 160–161. https://doi.org/10.35767/gscpgbull.38.1.153

Della Valle, R.S., 1975. Uranium mineralization in Lemhi County, Idaho; M.A. thesis, Queen's College, The City University of New York, New York, 125 p.

Derome, D., Cathelineau, M., Cuney, M., Fabre, C., Lhomme, T., and Banks, D.A., 2005. Mixing of sodic and calcic brines and uranium deposition at McArthur River, Saskatchewan, Canada: a raman and laser-induced breakdown spectroscopic study of fluid inclusions; Economic Geology, v. 100, no. 8, p. 1529–1545. https://doi.org/10.2113/gsecongeo.100.8.1529

Druschel, G.K. and Rosenberg, P.E., 2001. Non-magmatic fracture-controlled hydrothermal systems in the Idaho batholith: South Fork Payette geothermal system; Chemical Geology, v. 173, no. 4, p. 271–291. https://doi.org/10.1016/S0009-2541(00)00280-1

Dumond, G., Goncalves, P., Williams, M.L., and Jercinovic, M.J., 2010. Subhorizontal fabrics in exhumed continental lower crust and implications for lower crustal flow: Athabasca granulite terrane, western Canadian Shield; Tectonics, v. 29, no. 2, TC2006. https://doi.org/10.1029/2009TC002514

Dumond, G., Goncalves, P., Williams, M.L., and Jercinovic, M.J., 2015. Monazite as a monitor of melting, garnet growth and feldspar recrystallization in continental lower crust; Journal of Metamorphic Geology, v. 33, no. 7, p. 735–762. https://doi.org/10.1111/jmg.12150

Dyke, A.S. and Prest, V.K., 1987. Paleogeography of northern North America, 18 000 – 5 000 years ago; Geological Survey of Canada, Map 1703A, scale 1:12 500 000. https://doi.org/10.4095/133927

Dyke, A.S., Andrews, J.T., Clark, P.U., England, J.H., Miller, G.H., Shaw, J., and Veillette, J.J., 2002. The Laurentide and Innuitian ice sheets during the Last Glacial Maximum; Quaternary Science Reviews, v. 21, no. 1–3, p. 9–31. https://doi.org/10.1016/S0277-3791(01)00095-6

Farley, K.A., 2000. Helium diffusion from apatite: general behavior as illustrated by Durango fluorapatite; Journal of Geophysical Research: Solid Earth, v. 105, no. B2, p. 2903–2914. https://doi.org/10.1029/1999jb900348

Fehn, U., Cathles, L.M., and Holland, H.D., 1978. Hydrothermal convection and uranium deposits in abnormally radioactive plutons; Economic Geology, v. 73, no. 8, p. 1556–1566. https://doi.org/10.2113/gsecongeo.73.8.1556

Flowers, R.M., 2009. Exploiting radiation damage control on apatite (U – Th)/He dates in cratonic regions; Earth and Planetary Science Letters, v. 277, no. 1–2, p. 148–155. https://doi.org/10.1016/j.epsl.2008.10.005

Flowers, R.M., Mahan, K.H., Bowring, S.A., Williams, M.L., Pringle, M.S., and Hodges, K.V., 2006a. Multistage exhumation and juxtaposition of lower continental crust in the western Canadian Shield: linking high-resolution U-Pb and $^{40}Ar/^{39}Ar$ thermochronometry with pressure-temperature-deformation paths; Tectonics, v. 25, no. 4, TC4003. https://doi.org/10.1029/2005TC001912

Flowers, R.M., Bowring, S.A., and Reiners, P.W., 2006b. Low long-term erosion rates and extreme continental stability documented by ancient (U-Th)/He dates; Geology, v. 34, no. 11, p. 925–928. https://doi.org/10.1130/G22670A.1

Flowers, R.M., Ketcham, R.A., Shuster, D.L., and Farley, K.A., 2009. Apatite (U-Th)/He thermochronometry using a radiation damage accumulation and annealing model; Geochimica et Cosmochimica Acta, v. 73, no. 8, p. 2347–2365. https://doi.org/10.1016/j.gca.2009.01.015

Fuchs, H. and Hilger, W., 1989. Kiggavik (Lone Gull): an unconformity related uranium deposit in the Thelon basin, Northwest Territories, Canada; *in* Uranium resources and geology of North America; International Atomic Energy Agency, Technical Document, IAEA-TECDOC-500, p. 429–454.

Fuchs, H.D., Hilger, W., and Prosser, E., 1986. Geology and exploration history of the Lone Gull property; *in* Uranium deposits of Canada, (ed.) L. Evans; Canadian Institute of Mining and Metallurgy, Special Volume 33, p. 286–292.

Fyfe, W.S., 1973. The generation of batholiths; Tectonophysics, v. 17, p. 273–283. https://doi.org/10.1016/0040-1951(73)90007-3

Gautheron, C., Tassan-Got, L., Barbarand, J., and Pagel, M., 2009. Effect of alpha-damage annealing on apatite (U-Th)/He thermochronology; Chemical Geology, v. 266, no. 3–4, p. 157–170. https://doi.org/10.1016/j.chemgeo.2009.06.001

Gigon, J., Skirrow, R., Harlaux, M., Richard, A., Mercadier, J., Annesley, I.R., and Villeneuve, J., 2019. Insights into B-Mg-metasomatism at the Ranger U deposit (NT, Australia) and comparison with Canadian unconformity-related U deposits; Minerals, v. 9, no. 7, p. 432. https://doi.org/10.3390/min9070432

Guenthner, W.R., Reiners, P.W., Ketcham, R.A., Nasdala, L., and Giester, G., 2013. Helium diffusion in natural zircon: radiation damage, anisotropy, and the interpretation of zircon (U-Th)/He thermochronology; American Journal of Science, v. 313, no. 3, p. 145–198. https://doi.org/10.2475/03.2013.01

Hanmer, S., 1997. Geology of the Striding-Athabasca mylonitic zone, northern Saskatchewan and southeastern district of Mackenzie, Northwest Territories; Geological Survey of Canada, Bulletin 501, 92 p. https://doi.org/10.4095/209170

Hanmer, S., Ji, S., Darrach, M., and Kopf, C., 1991. Tantato Domain, northern Saskatchewan: a segment of the Snowbird tectonic zone; Geological Survey of Canada, Paper 91-1C, p. 121–133. https://doi.org/10.4095/132567

Hanmer, S., Darrach, M., and Kopf, C., 1992. The east Athbasca mylonite zone: an Archean segment of the Snowbird tectonic zone; Geological Survey of Canada, Paper 92-1C, p. 19–29. https://doi.org/10.4095/132845

Hanmer, S., Parrish, R., Williams, M., and Kopf, C., 1994. Striding-Athabasca mylonite zone: complex Archean deep-crustal deformation in the East Athabasca mylonite triangle, northern Saskatchewan; Canadian Journal of Earth Sciences, v. 31, no. 8, p. 1287–1300. https://doi.org/10.1139/e94-111

Hanmer, S., Williams, M., and Kopf, C., 1995. Striding Athabasca mylonite zone: implications for the Archean and Early Proterozoic tectonics of the western Canadian Shield; Canadian Journal of Earth Sciences, v. 32, no. 2, p. 178–196. https://doi.org/10.1139/e95-015

Hartlaub, R.P., Chacko, T., Heaman, L.M., Creaser, R.A., and Ashton, K.E., 2004. The Archean Murmac Bay Group: evidence for a giant Archean rift in the Rae Province; Precambrian Research, v. 131, p. 345–372.

Hartlaub, R.P., Chacko, T., Heaman, L.M., Creaser, R.A., Ashton, K.E., and Simonetti, A., 2005. Ancient (Meso- to Paleoarchean) crust in the Rae Province, Canada: evidence from Sm-Nd and U-Pb constraints; Precambrian Research, v. 141, no. 3–4, p. 137–153. https://doi.org/10.1016/j.precamres.2005.09.001

Hartlaub, R.P., Heaman, L.M., Chacko, T., and Ashton, K.E., 2007. Circa 2.3-Ga magmatism of the Arrowsmith Orogeny, Uranium City region, Western Churchill Craton, Canada; The Journal of Geology, v. 115, no. 2, p. 181–195. https://doi.org/10.1086/510641

Hasterok, D., Gard, M., and Webb, J., 2018. On the radiogenic heat production of metamorphic, igneous, and sedimentary rocks; Geoscience Frontiers, v. 9, no. 6, p. 1777–1794. https://doi.org/10.1016/j.gsf.2017.10.012

Hecht, L. and Cuney, M., 2000. Hydrothermal alteration of monazite in the Precambrian crystalline basement of the Athabasca Basin (Saskatchewan, Canada): implications for the formation of unconformity-related uranium deposits; Mineralium Deposita, v. 35, p. 791–795. https://doi.org/10.1007/s001260050280

Hendry, H.E. and Wheatley, K.L., 1985. The Carswell Formation, northern Saskatchewan: stratigraphy, sedimentology, and structure; *in* The Carswell structure uranium deposits, (ed.) R. Lainé, D. Alonso, and M. Svab; Geological Association of Canada, Special Paper 29, p. 87–103.

Henry, D.J., Novák, M., Hawthorne, F.C., Ertl, A., Dutrow, B.L., Uher, P., and Pezzotta, F., 2011. Nomenclature of the tourmaline-supergroup minerals; American Mineralogist, v. 96, p. 895–913. https://doi.org/10.2138/am.2011.3636

Hillacre, S., Ansdell, K., McEwan, B., Batty, M., Onstad, C., Johnson, J., Mohrbutter, R., and Cross, S., 2019. The giant Arrow uranium deposit, Patterson Lake corridor, Athabasca Basin: overview of present knowledge; Geological Association of Canada–Mineralogical Association of Canada, Volume of abstracts, v. 42, p. 109.

Hoeve, J. and Quirt, D., 1984. Mineralization and host rock alteration in relation to clay mineral diagenesis and evolution of the Middle-Proterozoic, Athabasca Basin, northern Saskatchewan, Canada; Saskatchewan Research Council, SRC Technical Report 187, 187 p.

Hoeve, J. and Sibbald, T.I., 1978. On the genesis of Rabbit Lake and other unconformity-type uranium deposits in northern Saskatchewan, Canada; Economic Geology, v. 73, no. 8, p. 1450–1473. https://doi.org/10.2113/gsecongeo.73.8.1450

Hyndman, D.W., 1981. Controls on source and depth of emplacement of granitic magma; Geology, v. 9, no. 6, p. 244–249. https://doi.org/10.1130/0091-7613(1981)9%3C244:COSADO%3E2.0.CO;2

Jaupert, C., Mareschal, J-C., and Iarotsky, L., 2016. Radiogenic heat production in the continental crust; Lithos, v. 262, p. 398–427. https://doi.org/10.1016/j.lithos.2016.07.017

Jeanneret, P., Goncalves, P., Durand, C., Poujol, M., Trap, P., Marquer, D., Quirt, D., and Ledru, P., 2017. Geochronological constraints on the trans-Hudsonian tectono-metamorphic evolution of the pre-Athabasca basement within the Wollaston-Mudjatik transition zone, Saskatchewan; Precambrian Research, v. 301, p. 152–178. https://doi.org/10.1016/j.precamres.2017.07.019

Jefferson, C.W., Thomas, D.J., Gandhi, S.S., Ramaekers, P., Delaney, G., Brisbin, D., Cutts, C., Portella, P., and Olson, R.A., 2007. Unconformity-associated uranium deposits of the Athabasca Basin, Saskatchewan and Alberta; *in* EXTECH IV: Geology and uranium EXploration TECHnology of the Proterozoic Athabasca Basin, Saskatchewan and Alberta, (ed.) C.W. Jefferson and G. Delaney; Geological Survey of Canada, Bulletin 588, p. 23–67. https://doi.org/10.4095/223744

Johnson, C.M., Beard, B.L., and Roden, E.E., 2008. The iron isotope fingerprints of redox and biogeochemical cycling in modern and ancient Earth; Annual Review of Earth Planet Sciences, v. 36, p. 457–493. https://doi.org/10.1146/annurev.earth.36.031207.124139

Johnstone, D., Bethune, K., and Tschirhart, V.T., 2019. The structural and lithological evolution of the Patterson Lake corridor, southwestern Athabasca Basin, Saskatchewan; Geological Association of Canada–Mineralogical Association of Canada Annual Conference, Volume of abstracts, v. 42, p. 117–118.

Kelly, C., Davis, W.J., Potter, E.G., and Corriveau, L., 2020. Geochemistry of hydrothermal tourmaline from IOCG occurrences in the Great Bear magmatic zone: implications for fluid source(s) and fluid composition evolution; Ore Geology Reviews, v. 118, 103329. https://doi.org/10.1016/j.oregeorev.2020.103329

Ketcham, R.A., 2005. Forward and inverse modeling of low-temperature thermochronometry data; Reviews in Mineralogy and Geochemistry, v. 58, no. 1, p. 275–314. https://doi.org/10.2138/rmg.2005.58.11

Koster, F. and Baadsgaard, H., 1970. On the geology and geochronology of northwestern Saskatchewan; Canadian Journal of Earth Sciences, v. 7, no. 3, p. 919–930. https://doi.org/10.1139/e70-087

Kotzer, T. and Kyser, T.K., 1995. Petrogenesis of the Proterozoic Athabasca basin, northern Saskatchewan, and its relation to diagenesis, hydrothermal uranium mineralization and paleohydrology; Chemical Geology, v. 120, p. 45–89. https://doi.org/10.1016/0009-2541(94)00114-N

Kuhns, R.J., 1980. Structural and chemical aspects of the Lochsa geothermal system near the northern margin of the Idaho batholith; M.Sc. thesis, Washington State University, Pullman, Washington, 121 p.

Kyser, T.K. and Cuney, M., 2009. Unconformity-related uranium deposits; *in* Recent and not-so-recent developments in uranium deposits and implications for exploration, (ed.) M. Cuney and T.K. Kyser; Mineralogical Association of Canada, Short Course Series, v. 39, p. 161–220.

Kyser, T.K. and Cuney, M., 2015. Basins and uranium and deposits; *in* Geology and geochemistry of uranium and thorium deposits, (ed.) T.K. Kyser and M. Cuney; Mineralogical Association of Canada, Short Course Series, v. 46, p. 225–304.

Kyser, T.K., Wilson, M.R., and Ruhrmann, G., 1989. Stable isotope constraints on the role of graphite in the genesis of unconformity-type uranium deposits; Canadian Journal of Earth Sciences, v. 26, no. 3, p. 490–498. https://doi.org/10.1139/e89-042

Landais, P., Dubessy, J., Dereppe, J.M., and Philp, R.P., 1993. Characterization of graphite alteration and bitumen genesis in the Cigar Lake deposit (Saskatchewan, Canada); Canadian Journal of Earth Sciences, v. 30, no. 4, p. 743–753. https://doi.org/10.1139/e93-060

Li, Z., Chi, G., and Bethune, K.M., 2016. The effects of basement faults on thermal convection and implications for the formation of unconformity-related uranium deposits in the Athabasca Basin, Canada; Geofluids, v. 16, no. 4, p. 729–751. https://doi.org/10.1111/gfl.12180

Liang, R., Chi, G., Ashton, K., Blamey, N., and Fayek, M., 2017. Fluid compositions and P-T conditions of vein-type uranium mineralization in the Beaverlodge uranium district, northern Saskatchewan, Canada; Ore Geology Reviews, v. 80, p. 460–483. https://doi.org/10.1016/j.oregeorev.2016.07.012

LeCheminant, A.N. and Heaman, L.M., 1989. Mackenzie igneous events, Canada: Middle Proterozoic hotspot magmatism associated with ocean opening; Earth and Planetary Science Letters, v. 96, no. 1–2, p. 38–48. https://doi.org/10.1016/0012-821X(89)90122-2

Ma, S.M., Kellett, D.A.-M., Godin, L., and Jercinovic, M., 2019. Localisation of the brittle Bathurst fault on pre-existing fabrics: a case for structural inheritance in the northeastern Slave craton, western Nunavut, Canada; Canadian Journal of Earth Sciences, e-First article. https://doi.org/10.1139/cjes-2019-0100

MacDonald, C., 1985. Mineralogy and geochemistry of the sub-Athabasca regolith near Wollaston Lake; *in* Geology of uranium deposits, (ed.) T.I.I. Sibbald and W. Petruk; Canadian Institute of Mining, Special Volume 32, p. 155–158.

Mahan, K.H., Goncalves, P., Flowers, R., Williams, M.L., and Hoffman-Setka, D., 2008. The role of heterogeneous strain in the development and preservation of a polymetamorphic record in high-P granulites, western Canadian Shield; Journal of Metamorphic Geology, v. 26, no. 6, p. 669–694. https://doi.org/10.1111/j.1525-1314.2008.00783.x

Marschall, H.R. and Jiang, S.-Y., 2011. Tourmaline isotopes: no element left behind; Elements, v. 7, p. 313–319. https://doi.org/10.2113/gselements.7.5.313

Marschall, H.R. and Foster, G.L., 2018. Boron isotopes in earth and planetary sciences – a short history and introduction; *in* Boron isotopes: the fifth element; Advances in isotope geochemistry, (ed.) H.R. Marschall and G.L. Foster; Springer International Publishing, p. 1–11https://doi.org/10.1007/978-3-319-64666-4_1

Martz, P., Mercadier, J., Cathelineau, M., Perret, J., Quirt, D., Doney, A., and Ledru, P., 2017. Multiple mineralizing events at the Cigar Lake deposit: an integrated-study of uranium oxide dating and geochemistry; *in* 14th biennial meeting of the Society for Geology Applied to Mineral Deposits, Proceedings, v. 2, p. 755–758.

Martz, P., Mercadier, J., Cathelineau, M., Boiron, M.-C., Quirt, D., Doney, A., Gerbeaud, O., De Wally, E., and Ledru, P., 2018. Formation of U-rich mineralizing fluids through basinal brine migration within basement hosted shear zones: A large-scale study of the fluid chemistry around the unconformity-related Cigar Lake U deposit (Saskatchewan, Canada); Chemical Geology, v. 508, p. 116–143. https://doi.org/10.1016/j.chemgeo.2018.05.042

McDonough, M.R., McNicoll, V.J., Schetselaar, E.M., and Grover, T.W., 2000. Geochronological and kinematic constraints on crustal shortening and escape in a two-sided oblique-slip collisional and magmatic orogen, Paleoproterozoic Taltson magmatic zone, northeastern Alberta; Canadian Journal of Earth Sciences, v. 37, no. 11, p. 1549–1573. https://doi.org/10.1139/e00-089

McLaren, S., Sandiford, M., and Hand, M., 1999. High radiogenic heat–producing granites and metamorphism — an example from the western Mount Isa inlier, Australia; Geology, v. 27, no. 8, p. 679–682.https://doi.org/10.1130/0091-7613(1999)027%3C0679:HRHPGA%3E2.3.CO;2

McKechnie, C.L., Annesley, I.R., and Ansdell, K.M., 2013. Geological setting, petrology, and geochemistry of granitic pegmatites and leucogranites hosting U-Th-REE mineralization at Fraser Lakes Zone B, Wollaston Domain, northern Saskatchewan, Canada; *in* Uranium in Canada: geological environments and exploration developments, (ed.) E.G. Potter, D. Quirt, and C.W. Jefferson; Exploration and Mining Geology, v. 21, p. 1–26.

McNeice, G.M. and Jones, A.G., 2001. Multisite, multi-frequency tensor decomposition of magnetotelluric data; Geophysics, v. 66, no. 1, p. 158–173. https://doi.org/10.1190/1.1444891

McNicoll, V.J., Theriault, R.J., and McDonough, M.R., 2000. Taltson basement gneissic rocks: U-Pb and Nd isotopic constraints on the basement of the Paleoproterozoic Taltson magmatic zone, northeastern Alberta; Canadian Journal of Earth Sciences, v. 37, no. 11, p. 1575–1596. https://doi.org/10.1139/e00-034

Mercadier, J., Richard, A., Boiron, M.-C., Cathelineau, M., and Cuney, M., 2010. Migration of brines in the basement rocks of the Athabasca Basin through microfracture networks (P-Patch U deposit, Canada); Lithos, v. 115, no. 1–4, p. 121–136. https://doi.org/10.1016/j.lithos.2009.11.010

Mercadier, J., Richard, A., and Cathelineau, M., 2012. Boron-and magnesium-rich marine brines at the origin of giant unconformity-related uranium deposits: $\delta^{11}B$ evidence from Mg-tourmalines; Geology, v. 40, no. 3, p. 231–234. https://doi.org/10.1130/G32509.1

Mercadier, J., Annesley, I.R., McKechnie, C.L., Bogdan, T.S., and Creighton, S., 2013. Magmatic and metamorphic uraninite mineralization in the western margin of the Trans-Hudson orogen, Saskatchewan, Canada: a uranium source for unconformity-related uranium deposits?; Economic Geology, v. 108, no. 5, p. 1037–1065. https://doi.org/10.2113/econgeo.108.5.1037

Metz, M.C., Brookins, D.G., Rosenberg, P.E., and Zartman, R.E., 1985. Geology and geochemistry of the Snowbird deposit, Mineral County, Montana; Economic Geology, v. 80, no. 2, p. 394–409. https://doi.org/10.2113/gsecongeo.80.2.394

Miller, A.R., Blackwell, J.D., Curtis, L., Hilger, W., McMillan, R.H., and Nutter, E., 1984. Geology and discovery of Proterozoic uranium deposits, central District of Keewatin, Northwest Territories; International Atomic Energy Agency, Technical Document, TC315, p. 285–312.

Morelli, R.M., Hartlaub, R.P., Ashton, K.E., and Ansdell, K.M., 2009. Evidence for enrichment of subcontinental lithospheric mantle from Paleoproterozoic intracratonic magmas: geochemistry and U – Pb geochronology of Martin Group igneous rocks, western Rae Craton, Canada; Precambrian Research, v. 175, p. 1–15. https://doi.org/10.1016/j.precamres.2009.04.005

Mount, S.A., 2019. Iron isotope fractionation within the Patterson Lake corridor uranium deposits; H.B.Sc thesis, Carleton University, Ottawa, Ontario, 72 p.

Natural Resources Canada, 2017. Geoscience data repository: aeromagnetic data. <http://gdr.agg.nrcan.gc.ca> [accessed August 1, 2018]

Natural Resources Canada, 2019. Geoscience data repository: gravity data. <http://gdr.agg.nrcan.gc.ca> [accessed September 2, 2019]

Pagel, M., 1975. Détermination des conditions physico-chimiques de la silicification diagénétique des grès Athasbasca (Canada) au moyen des inclusions fluides; Comptes Rendus de l'Académie des Sciences, Paris, v. 280, p. 2301–2304.

Pană, D., Creaser, R.A., Muehlenbachs, K., and Wheatley, K, 2007. Basement geology in the Alberta portion of the Athabasca Basin: context for the Maybelle River area; *in* EXTECH IV: Geology and Uranium EXploration TECHnology of the Proterozoic Athabasca Basin, Saskatchewan and Alberta, (ed.) C.W. Jefferson and G. Delaney; Geological Survey of Canada, Bulletin 588, p. 135–153. https://doi.org/10.4095/223749

Peterson, T.D. and van Breemen, O., 1999. Review and progress report of Proterozoic granitoid rocks of the Western Churchill Province, Northwest Territories (Nunavut); *in* Current Research 1990-C, Geological Survey of Canada, p. 119–127. https://doi.org/10.4095/210177

Peterson, T.D., van Breemen, O., Sandeman, H., and Cousens, B., 2002. Proterozoic (1.85 - 1.75 Ga) igneous suites of the Western Churchill Province: granitoid and ultrapotassic magmatism in a reworked Archean hinterland; Precambrian Research, v. 119, no. 1–4, p. 73–100. https://doi.org/10.1016/S0301-9268(02)00118-3

Peterson, T.D., Pehrsson, S., Martel, E., and Percival, J., in press. Lithogeochemical and Sm-Nd isotopic data for the GEM2/South Rae study area, 2012–2016; Geological Survey of Canada, Open File 8510, 1 zip file.

Polyakov, V.B. and Soultanov, D.M., 2011. New data on equilibrium iron isotope fractionation among sulfides: Constraints on mechanisms of sulfide formation in hydrothermal and igneous systems; Geochimica et Cosmochimica Acta, v. 75, no. 7, p. 1957–1974. https://doi.org/10.1016/j.gca.2011.01.019

Potter, E.G., Sharpe, R., Girard, I., Fayek, M., Gammon, P., Quirt, D., and Robbins, J., 2015. Fe and Mg signatures of the Bong uranium deposit, Thelon Basin, Nunavut; *in* Targeted Geoscience Initiative 4: unconformity-related uranium systems, (ed.) E.G. Potter and D.M. Wright; Geological Survey of Canada, Open File 7791, p. 52–60. https://doi.org/10.4095/295783

Potter, E.G., Tschirhart, V., Powell, J.W., Rabiei, M., Johnstone, D., Kelly, C., Pehrsson, S., Chi, G., Bethune, K., Craven, J., McEwen, B., Card, C., Bosman, S., Ashley, R., Frostad, S., MacKay, C., Ledru, P., Pană, D., and Wheatley, K., 2019. Formation of unconformity-related uranium deposits: insights from integrated multidisciplinary studies of the Patterson Lake corridor, northern Saskatchewan; *in* Open House 2019 Abstract Volume, Saskatchewan Ministry of Energy and Resources, Saskatchewan Geological Survey, Miscellaneous Report 2019-3, 3 p.

Poty, B. and Pagel, M., 1988. Fluid inclusions related to uranium deposits: a review; Journal of the Geological Society, v. 145, p. 157–162. https://doi.org/10.1144/gsjgs.145.1.0157

Powell, J.W., Pană, D., Card, C.D., Potter, E.G., Tschirhart, V., and Joyce, N., 2018a. New geochronological insights into the Taltson Domain of northern Alberta and Saskatchewan; *in* Targeted Geoscience Initiative: 2017 report of activities, volume 2, (ed.) N. Rogers; Geological Survey of Canada, Open File 8373, p. 43–56. https://doi.org/10.4095/306600

Powell, J.W., Tschirhart, V., Potter, E.G., Card, C.D., Pană, D.I., Wheatley, K., and MacKay, C., 2018b. Integrated geochronological, geophysical and isotopic investigation in the Patterson Lake corridor of the southwestern Athabasca Basin, Canada; 15th Quadrennial International Association on the Genesis of Ore Deposits Symposium, Salta Argentina, Proceedings, p. 319–320.

Powell, J.W., Potter, E.G., Pehrsson, S.J., and Tschirhart, V., 2019a. Deciphering complex, multi-episodic thermal histories from cratonic interiors through low-temperature thermochronology: a case study from the Paleo- to Mesoproterozoic Athabasca Basin of northern Canada; American Geophysical Union (AGU) 2019, December 9–13, San Francisco, U.S.A. (abstract).

Powell, J.W., Potter, E.G., Tschirhart, V., Percival, J.B., Mount, S., McEwan, B., Ashley, R., and Wheatley, K., 2019b. Quantifying fertile alteration in the Patterson Lake corridor, Saskatchewan, through visible-near infrared-shortwave infrared spectroscopy; *in* Targeted Geoscience Initiative: 2018 report of activities, (ed.) N. Rogers; Geological Survey of Canada, Open File 8549, p. 365–379. https://doi.org/10.4095/313671

Prest, V.K., 1984. The Late Wisconsinan glacier complex; *in* Quaternary stratigraphy of Canada – a Canadian contribution to the IGCP project 24, (ed.) R.J. Fulton; Geological Survey of Canada, Paper 84-10, p. 21–36. https://doi.org/10.4095/119756

Prest, V.K., Grant, D.R., and Rampton, V.N., 1968. Glacial map of Canada; Geological Survey of Canada, Map 1253A, scale 1:5 000 000. https://doi.org/10.4095/108979

Rabiei, M., Chi, G., Potter, E.G., Tschirhart, V., MacKay, C., Frostad, S., McElroy, R., and Ashley, R., 2018. Characterization of fluids associated with uranium mineralization in the Patterson Lake area: a preliminary fluid inclusion study; RFG 2018: Resources for Future Generations, June 16–21, 2018, Abstract 1567, p. 149.

Rabiei, M., Chi, G., Potter, E.G., Tschirhart, V., Feng, R., MacKay, C., Frostad, S., McElroy, R., Ashley, R., and McEwan, B., 2019. Evolution of hydrothermal fluids in the Patterson Lake corridor, southwestern Athabasca Basin: significance for uranium mineralization; Geological Association of Canada–Mineralogical Association of Canada (GAC-MAC) Annual Conference, Volume of abstracts, v. 42, p. 163.

Rainbird, R.H. and Young, G.M., 2009. Colossal rivers, massive mountains and supercontinents; Earth, v. 54, no. 4, p. 52–61.

Rainbird, R.H., Stern, R.A., Rayner, N., and Jefferson, C.W., 2007. Age, provenance, and regional correlation of the Athabasca Group, Saskatchewan and Alberta, constrained by igneous and detrital zircon geochronology; *in* EXTECH IV: Geology and Uranium EXploration TECHnology of the Proterozoic Athabasca Basin, Saskatchewan and Alberta, (ed.) C.W. Jefferson and G. Delaney; Geological Survey of Canada, Bulletin 588, p. 193–209. https://doi.org/10.4095/223761

Ramaekers, P., Jefferson, C.W., Yeo, G.M., Collier, B., Long, D.G.F., Drever, G., McHardy, S., Jiricka, D., Cutts, C., Wheatley, K., Catuneanu, O., Bernier, S., Kupsch, B., and Post, R.T., 2007. Revised geological map and stratigraphy of the Athabasca group, Saskatchewan and Alberta; *in* EXTECH IV: Geology and Uranium EXploration TECHnology of the Proterozoic Athabasca Basin, Saskatchewan and Alberta, (ed.) C.W. Jefferson and G. Delaney; Geological Survey of Canada, Bulletin 588, p. 155–191. https://doi.org/10.4095/223754

Ramaekers, P., McElroy, R., and Cataneanu, O., 2017. Mid-Proterozoic continental extension as a control on Athabasca region uranium emplacement, Saskatchewan and Alberta, Canada; Proceedings of the 14th SGA Biennial Meeting, Québec City, Quebec, 20–23 August 2017, p. 759–762 (abstract).

Regan, S.P., Williams, M.L., Leslie, S., Mahan, K.H., Jercinovic, M.J., and Holland, M.E., 2014. The Cora Lake shear zone Athabasca granulite terrane, an intraplate response to far-field orogenic processes during the amalgamation of Laurentia; Canadian Journal of Earth Sciences, v. 51, no. 9, p. 877–911. https://doi.org/10.1139/cjes-2014-0015

Richard, A., Pettke, T., Cathelineau, M., Boiron, M.-C., Mercadier, J., Cuney, M., and Derome, D., 2010. Brine–rock interaction in the Athabasca basement (McArthur River U deposit, Canada): consequences for fluid chemistry and uranium uptake; Terra Nova, v. 22, no. 4, p. 303–308. https://doi.org/10.1111/j.1365-3121.2010.00947.x

Richard, A., Rozsypal, C., Mercadier, J., Banks, D.A., Cuney, M., Boiron, M.-C., and Cathelineau, M., 2012. Giant uranium deposits formed from exceptionally uranium-rich acidic brines; Nature Geoscience, v. 5, p. 142–146. https://doi.org/10.1038/ngeo1338

Richard, A., Boulvais, P., Mercadier, J., Boiron, M.-C., Cathelineau, M., Cuney, M., and France-Lanord, C., 2013. From evaporated seawater to uranium-mineralizing brines: Isotopic and trace element study of quartz–dolomite veins in the Athabasca system; Geochimica et Cosmochimica Acta, v. 113, p. 38–59. http://dx.doi.org/10.1016/j.gca.2013.03.009

Richard, A., Cathelineau, M., Boiron, M.-C., Mercadier, J., Banks, D.A., and Cuney, M., 2016. Metal-rich fluid inclusions provide new insights into unconformity-related U deposits (Athabasca Basin and Basement, Canada); Mineralium Deposita, v. 51, p. 249–270. https://doi.org/10.1007/s00126-015-0601-4

Reiners, P.W. and Brandon, M.T., 2006. Using thermochronology to understand orogenic erosion; Annual Review of Earth and Planetary Sciences, v. 34, p. 419–466. https://doi.org/10.1146/annurev.earth.34.031405.125202

Reiners, P.W., Farley, K.A., and Hickes, H.J., 2002. He diffusion and (U-Th)/He thermochronometry of zircon: initial results from Fish Canyon Tuff and Gold Butte; Tectonophysics, v. 349, no. 1–4, p. 297–308. https://doi.org/10.1016/S0040-1951(02)00058-6

Rosenberg, P.E. and Foit, F.F., Jr., 2006. Magnesiofoitite from the uranium deposits of the Athabasca Basin, Saskatchewan, Canada; The Canadian Mineralogist, v. 44, no. 4, p. 959–965. http://dx.doi.org/10.2113/gscanmin.44.4.959

Ross, D.A., 2015. Technical report on the Patterson Lake South property, northern Saskatchewan, Canada; NI 43-101 report by RPA Inc. for Fission Uranium Corp., 140 p.

Ross, G.M., 2002. Evolution of Precambrian continental lithosphere in Western Canada: results from Lithoprobe studies in Alberta and beyond; Canadian Journal of Earth Sciences, v. 39, no. 3, p. 413–437. https://doi.org/10.1139/E02-012

Ross, G.M., Eaton, D.W., Boerner, D.E., and Miles, W., 2000. Tectonic entrapment and its role in the evolution of the continental lithosphere: an example from the Precambrian of western Canada; Tectonics, v. 19, p. 116–134. https://doi.org/10.1029/1999tc900047

Rouxel, O., Dobbek, N., Ludden, J., and Fouquet, Y., 2003. Iron isotope fractionation during oceanic crust alteration; Chemical Geology v. 202, p. 155–182. https://doi.org/10.1016/j.chemgeo.2003.08.011

Rouxel, O., Fouquet, Y., and Ludden, J.N., 2004. Subsurface processes at the Lucky Strike hydrothermal field, Mid-Atlantic Ridge: evidence from sulfur, selenium, and iron isotopes; Geochemica et Cosmochimica Acta, v. 68, no. 10, p. 2295–2311. https://doi.org/10.1016/j.gca.2003.11.029

Rouxel, O., Shanks, W.C., III, Bach, W., and Edwards, K.J., 2008. Integrated Fe- and S-isotope study of seafloor hydrothermal vents at East Pacific Rise 9–10°N; Chemical Geology, v. 252, no. 3–4, p. 214–227. https://doi.org/10.1016/j.chemgeo.2008.03.009

Rukhlov, A.S., 2011. Review of metallic mineralization in Alberta with emphasis on gold potential; Energy Resources Conservation Board, ERCB/AGS Open File Report 2011-01, 93 p.

Rybach, L., 1988. Determination of heat production rate; *in* Handbook of terrestrial heat-flow density determination; Solid Earth Sciences Library, volume 4, (ed.) R. Haenel, L. Rybach, and L. Stegena; Kluwer Academic Press, p. 125–142. https://doi.org/10.1007/978-94-009-2847-3

Samson, I.M., Wood, S.A., and Finucane, K., 2004. Fluid inclusion characteristics and genesis of the fluorite-parisite mineralization in the Snowbird deposit, Montana; Economic Geology, v. 99, p. 1727–1744. https://doi.org/10.2113/gsecongeo.99.8.1727

Sangély, L., Chaussidon, M., Michels, R., Brouand, M., Cuney, M., Huault, V., and Landais, P., 2007. Micrometer scale carbon isotopic study of bitumen associated with Athabasca uranium deposits: constraints on the genetic relationship with petroleum source-rocks and the abiogenic origin hypothesis; Earth and Planetary Science Letters, v. 258, no. 3–4, p. 378–396. https://doi.org/10.1016/j.epsl.2007.03.018

Scott, J.M.J., 2012. Paleoproterozoic (1.75 Ga) granitoid rocks and uranium mineralization in the Baker Lake–Thelon Basin region, Nunavut; M.Sc. thesis, Carleton University, Ottawa, Ontario, 149 p.

Scott, J.M.J., Peterson, T.D., Davis, W.J., Jefferson, C.W., and Cousens, B.L., 2015. Petrology and geochronology of Paleoproterozoic intrusive rocks, Kiggavik uranium camp, Nunavut; Canadian Journal of Earth Sciences, v. 52, no. 7, p. 495–518. https://doi.org/10.1139/cjes-2014-0153

Scott, T.B., Riba Tort, O., and Allen, G.C., 2007. Aqueous uptake of uranium onto pyrite surfaces; reactivity of fresh versus weathered material; Geochimica et Cosmochimica Acta, v. 71, no. 21, p. 5044–5053. https://doi.org/10.1016/j.gca.2007.08.017

Severmann, S., Johnson, C.M., Beard, B.L., German, C.R., Edmonds, H.N., Chiba, H., and Green, D.R.H., 2004. The effect of plume processes on the Fe isotope composition of hydrothermally derived Fe in the deep ocean as inferred from the Rainbow vent site, Mid-Atlantic Ridge, 36°14′N; Earth and Planetary Science Letters, v. 225, no. 1–2, p. 63–76. https://doi.org/10.1016/j.epsl.2004.06.001

Shabaga, B.M., Fayek, M., Quirt, D., Jefferson, C.W., and Camacho, A., 2017. Mineralogy, geochronology, and genesis of the Andrew Lake uranium deposit, Thelon Basin, Nunavut, Canada; Canadian Journal of Earth Sciences, v. 54, no. 8, p. 850–868. https://doi.org/10.1139/cjes-2017-0024

Sibbald, T.I.I., 1974. La Loche (north) area: reconnaissance geological survey of the 74-C-NW and 74-C-NE; *in* Summary of Investigations 1974; Saskatchewan Department of Mines and Resources, Saskatchewan Geological Survey, p. 38–45.

Sibson, R.H., 1987. Earthquake rupturing as a mineralizing agent in hydrothermal systems; Geology, v. 15, no. 8, p. 701–704. https://doi.org/10.1130/0091-7613(1987)15%3C701:ERAAMA%3E2.0.CO;2

Sibson, R.H., 1990. Conditions for fault-valve behaviour; *in* Deformation mechanisms, rheology and tectonics, (ed.) R.J. Knipe and E.H. Rutter; Geological Society of London, Special Publication No. 54, p. 15–28.

Sibson, R.H., Robert, F., and Poulsen, K.H., 1988. High angle reverse faults, fluid pressure cycling, and mesothermal gold-quartz deposits; Geology, v. 16, no. 6, p. 551–555. https://doi.org/10.1130/0091-7613(1988)016%3C0551:HARFFP%3E2.3.CO;2

Snoeyenbos, D.R., Williams, M.L., and Hanmer, S., 1997. Archean high pressure metamorphism in the western Canadian Shield; European Journal of Mineralogy, v. 7, no. 6, p. 1251–1272. https://dx.doi.org/10.1127/ejm/7/6/1251

Spratt, J. E., Skulski, T., Craven, J.A., Jones, A.G., Snyder, D.B., and Kiyan, D., 2014. Magnetotelluric investigations of the lithosphere beneath the central Rae craton, mainland Nunavut, Canada; Journal of Geophysical Research–Solid Earth, v. 119, no. 3, p. 2415–2439. https://doi.org/10.1002/2013JB010221

Staatz, M.H., 1972. Geology and description of the thorium-bearing veins, Lemhi Pass Quadrangle, Idaho and Montana; U.S. Geological Survey, Bulletin 1351, p. 1–94.

Stasiuk, L.D., Sweet, A.R., and Issler, D.R., 2006. Reconstruction of burial history of eroded Mesozoic strata using kimberlite shale xenoliths, volcaniclastic and crater facies, Northwest Territories, Canada; International Journal of Coal Geology, v. 65, no. 1–3, p. 129–145. http://doi.org/10.1016/j.coal.2005.04.011

Stern, R.A., 1997. The GSC sensitive high resolution ion microprobe (SHRIMP): analytical techniques of zircon U-Th-Pb age determinations and performance evaluation; *in* Radiogenic age and isotope studies: report 10; Geological Survey of Canada, Current Research 1997-F, p. 1–31. https://doi.org/10.4095/209089

Stern, R.A. and Amelin, Y., 2003. Assessment of errors in SIMS zircon U-Pb geochronology using a natural zircon standard and NIST SRM 610 glass; Chemical Geology, v. 197, no. 1–4, p. 111–146. https://doi.org/10.1016/S0009-2541(02)00320-0

Stern, R.A., Card, C.D., Pană, D., and Rayner, N.M., 2003. SHRIMP U-Pb ages of granitoid basement rocks of the southwestern part of the Athabasca Basin, Saskatchewan and Alberta; Geological Survey of Canada, Current Research 2003-F3, 20 p. https://doi.org/10.4095/214595

Taylor, P.D.P., Maeck, R., and De Bièvre, P., 1992. Determination of the absolute isotopic composition and atomic weight of a reference sample of natural iron; International Journal of Mass Spectrometry and Ion Processes, v. 121, p. 111–125. https://doi.org/10.1016/0168-1176(92)80075-C

Thomas, D.J., 1983. Distribution, geological controls and genesis of uraniferous pegmatites in the Cree Lake zone of northern Saskatchewan; M.Sc. thesis, University of Regina, Regina, Saskatchewan, 213 p.

Tschirhart, V., Craven, J., Potter, E.G., Powell, J., Pehrsson, S., and McEwan, B., 2019. Preliminary modelling of MT data in the Patterson Lake corridor, Saskatchewan, Canada; 16th Biennial SAGA Conference & Exhibition, October 6–9, Durban, Extended abstracts, 3 p.

Tschirhart, V., Pehrsson, S., Card, C., Potter, E.G., Powell, J., and Pană, D., 2020. Interpretation of buried basement in the southwestern Athabasca Basin, Canada, from integrated geophysical and geological datasets; Geochemistry: Exploration, Environment, Analysis. https://doi.org/10.1144/geochem2019-061

Tornos, F., Wiedenbeck, M., and Velasco, F., 2012. The boron isotope geochemistry of tourmaline-rich alteration in the IOCG systems of northern Chile: implications for a magmatic-hydrothermal origin; Mineralium Deposita, v. 47, no. 5, p. 483–499. https://doi.org/10.1007/s00126-011-0383-2

Vance, D.B., 1986. The geology and geochemistry of three hot spring systems in the Shoup geothermal area, Lemhi County, Idaho; M.Sc. thesis, Washington State University, Pullman, Washington, 166 p.

van Hinsberg, V.J. and Marschall, H.R., 2007. Boron isotope and light element sector zoning in tourmaline: implications for the formation of B-isotopic signatures; Chemical Geology, v. 238, no. 3–4, p. 141–148. https://doi.org/10.1016/j.chemgeo.2006.11.002

van Hinsberg, V.J., Henry, D.J., and Marschall, H.R., 2011. Tourmaline: an ideal indicator of its host environment; The Canadian Mineralogist, v. 49, no. 1, p. 1–16. http://dx.doi.org/10.3749/canmin.49.1.1

van Middlesworth, P.E. and Wood, S.A., 1998. The aqueous geochemistry of the rare earth elements and yttrium. Part 7. REE, Th and U contents in thermal springs associated with the Idaho batholith; Applied Geochemistry, v. 13, no. 7, p. 861–884. https://doi.org/10.1016/S0883-2927(98)00019-5

van Schmus, W.R., Persons, S.S., Macdonald, R., and Sibbald, T.I.I., 1986. Preliminary results from U–Pb zircon geochronology of the Uranium City region, northwest Saskatchewan; *in* Summary of Investigations 1986; Saskatchewan Energy and Mines, Saskatchewan Geological Survey, Miscellaneous Report 86-4, p. 108–111.

Wang, K., Chi, G., Bethune, K.M., Li, Z., Blamey, N., Card, C., Potter, E.G., and Liu, Y., 2018. Fluid P-T-X characteristics and evidence for boiling in the formation of the Phoenix uranium deposit (Athabasca Basin, Canada): implications for unconformity-related uranium mineralization mechanisms; Ore Geology Reviews, v. 101, p. 122–142. https://doi.org/10.1016/j.oregeorev.2018.07.010

Weyer, H.J., 1992. Die Uranlagerstätte Kiggavik, Nordwestterritorien, Kanada; approved dissertation, Rheinisch-Westfälischien Technischen Hochschule, Aachen, Germany, 212 p.

Weyer, H.J., Friedrich, G., Bechtel, A., and Ballhorn, R.K., 1989. The Lone Gull uranium deposit: new geochemical and petrological data as evidence for the nature of the ore bearing solutions; International Atomic Energy Agency, Technical report, TC542/19, p. 293–306.

Whalen, J.B., Currie, K.L., and Chappell, B.W., 1987. A-type granites: geochemical characteristics, discrimination and petrogenesis; Contributions to Mineralogy and Petrology, v. 95, p. 407–419. https://doi.org/10.1007/BF00402202

Wilson, N.S.F., Stasiuk, L.D., and Fowler, M.G., 2002. Post-mineralization origin of organic matter in Athabasca unconformity uranium deposits, Saskatchewan; *in* Summary of Investigations 2002; Saskatchewan Industry and Resources, Saskatchewan Geological Survey, Miscellaneous Report 2002-4.2, p. 1–6.

Wilson, N.S.F., Stasiuk, L.D., and Fowler, M.G., 2007. Origin of organic matter in the Proterozoic Athabasca Basin of Saskatchewan and Alberta, and significance to unconformity uranium deposits; *in* EXTECH IV: Geology and Uranium EXploration TECHnology of the Proterozoic Athabasca Basin, Saskatchewan and Alberta, (ed.) C.W. Jefferson and G. Delaney; Geological Survey of Canada, Bulletin 588, p. 325–339. https://doi.org/10.4095/223778

Wolfe, M.R. and Stockli, D.F., 2010. Zircon (U-Th)/He thermochronometry in the KTB drill hole, Germany, and its implications for bulk He diffusion kinetics in zircon; Earth and Planetary Science Letters, v. 295, no. 1–2, p. 69–82. https://doi.org/10.1016/j.epsl.2010.03.025

Young, H.W., 1985. Geochemistry and hydrology of thermal springs in the Idaho Batholith and adjacent areas, central Idaho; U.S. Geological Survey, Water-Resources Investigations Report 85-4172, 44 p. https://doi.org/10.3133/wri854172